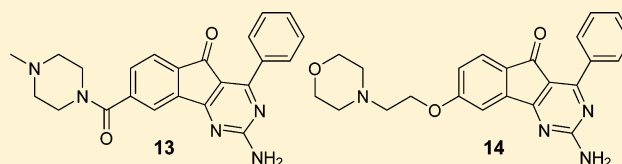


Design and Characterization of Optimized Adenosine A_{2A}/A₁ Receptor Antagonists for the Treatment of Parkinson's Disease

Brian C. Shook,* Stefanie Rassnick, Nathaniel Wallace, Jeffrey Crooke, Mark Ault, Devraj Chakravarty, J. Kent Barbay, Aihua Wang, Mark T. Powell, Kristi Leonard, Vernon Alford, Robert H. Scannevin, Karen Carroll, Lisa Lampron, Lori Westover, Heng-Keang Lim, Ronald Russell, Shawn Branum, Kenneth M. Wells, Sandra Damon, Scott Youells, Xun Li, Derek A. Beauchamp, Kenneth Rhodes, and Paul F. Jackson

Janssen Research and Development, L.L.C., Welsh and McKean Roads, P.O. Box 776, Spring House, Pennsylvania 19477, United States

ABSTRACT: The design and characterization of two, dual adenosine A_{2A}/A₁ receptor antagonists in several animal models of Parkinson's disease is described. Compound **1** was previously reported as a potential treatment for Parkinson's disease. Further characterization of **1** revealed that it was metabolized to reactive intermediates that caused the genotoxicity of **1** in the Ames and mouse lymphoma L51784 assays. The identification of the metabolites enabled the preparation of two optimized compounds **13** and **14** that were devoid of the metabolic liabilities associated with **1**. Compounds **13** and **14** are potent dual A_{2A}/A₁ receptor antagonists that have excellent activity, after oral administration, across a number of animal models of Parkinson's disease including mouse and rat models of haloperidol-induced catalepsy, mouse and rat models of reserpine-induced akinesia, and the rat 6-hydroxydopamine (6-OHDA) lesion model of drug-induced rotation.



■ INTRODUCTION

Parkinson's disease (PD) is a chronic, progressive neurodegenerative disease that is characterized by progressive impairment in motor function that is often accompanied by anxiety, depression, and cognitive impairment.¹ The majority of motor impairments of PD are caused by a gradual loss of dopamine-producing neurons in the ventral midbrain and concomitant loss of dopamine (DA) input to forebrain (striatal) motor structures.^{2,3} The cellular mechanisms underlying the relatively selective loss of midbrain DA neurons remains poorly understood. The loss of DA input to the neostriatum leads to dysregulation of striatal function and the classic motor symptoms of PD, such as resting tremor, muscular rigidity, akinesia, and bradykinesia. Although the loss of striatal DA precipitates many of the classical motor symptoms of PD, chronic neurodegeneration and inflammatory processes also affect other brain regions. Degenerative processes in these regions are likely to underlie the depression, cognitive impairment, and postural/gait instability in PD patients.

Understanding the loss of dopaminergic cells led to the majority of treatments that restore DA signaling and thereby reduce the severity of the motor symptoms. DA replacement therapy using levodopamine (L-DOPA), the precursor to DA, remains the gold-standard treatment for PD. Other approaches include inhibition of DA turnover using monoamine oxidase type B (MAO-B) inhibitors,⁴ catechol O-methyl-transferase (COMT) inhibitors,⁵ and inhibition of DA reuptake⁶ or direct agonists⁷ of postsynaptic DA receptors. Although the DA-

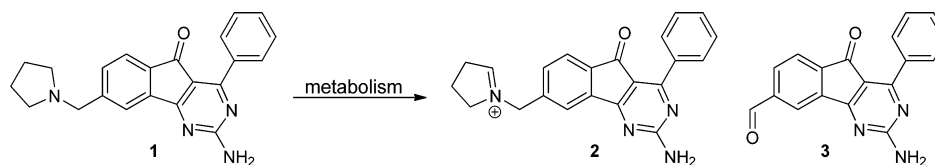
targeted therapies work well to address the PD-related motor disturbances, they all produce undesirable side effects (dyskinesia, hallucinations, and on-off effects) that become more severe and problematic with continued treatment. The aforementioned therapies typically show reduced efficacy as motor functions deteriorate and the disease progresses. Moreover, these treatments do not alter disease progression and do not address the comorbidities associated with PD including mood, postural instability, or cognitive disturbances. These comorbidities stem from progressive neurodegeneration in non-DA brain systems and therefore are not amenable to treatment with agents targeting DA signaling.

The limitations of DA replacement agents initiated non-DA-based approaches for the treatment of PD. One attractive nondopaminergic strategy that has been widely targeted is the modulation of adenosine receptors.⁸ Adenosine is a purine nucleotide produced by all metabolically active cells. Unlike classical neurotransmitters in the brain, adenosine is not packaged into vesicles or released from axon terminals in a Ca²⁺-dependent manner. Rather, extracellular adenosine in brain is derived from degradation of other purine nucleotides and from intracellular adenosine released via transmembrane transport.⁹ Adenosine acts as a neuromodulator that coordinates responses to DA and other neurotransmitters in areas of the brain that are responsible for motor function, learning, and memory.⁹ Adenosine exerts a tonic inhibitory

Received: December 2, 2011

Published: January 12, 2012

Scheme 1. Metabolism of Compound 1



effect of DA receptor signaling in forebrain motor and limbic structures. Adenosine is comprised of four distinct receptor subtypes designated A_{1} , A_{2A} , A_{2B} , and A_{3} belonging to the G protein-coupled receptor superfamily.¹⁰ A_{1} and A_{3} receptors are coupled to inhibitory G proteins, while A_{2A} and A_{2B} receptors are coupled to stimulatory G proteins. On the basis of in situ hybridization histochemistry and quantitative receptor autoradiography, the greatest densities of A_{2A} receptor expression in rodent brain are found in the neostriatum with lower levels in olfactory, neocortical, and limbic system structures.¹¹ On the basis of [^{11}C]-TMSX positron emission tomography (PET) imaging in human subjects and on autoradiographic studies of postmortem brain sections, the distribution of A_{2A} receptors in human brain closely matches the distribution in rodent brain, with a high concentration in the neostriatum and much lower levels in other brain regions.¹²

The loss of DA input into the neostriatum is a hallmark of PD and underlies many of the cardinal motor symptoms of this disorder. Also, it has been reported that overexpression of A_{2A} receptors correlates with the motor symptoms in PD.¹³ Adenosine A_{2A} receptors colocalize and physically associate with D_2 receptors in the striatum.^{2,3} A_{2A} and D_2 receptors have opposing effects on adenylate cyclase and cyclic adenosine monophosphate (cAMP) production in cells, such that activation of A_{2A} receptors inhibits D_2 receptor signaling. Conversely, A_{2A} receptor antagonists enhance D_2 -dependent signaling as shown by induction of immediate early gene *c-fos* expression in the striatopallidal pathway¹⁴ and facilitate other D_2 -mediated responses. Of importance to PD, pharmacological blockade of A_{2A} receptors has shown dramatic beneficial effects in preclinical animal models of PD,¹⁵ reversing haloperidol-induced catalepsy, showing potentiation of DA-mediated responses in DA-depleted [6-hydroxydopamine (6-OHDA)-treated] animals and dramatic relief of parkinsonian symptoms in 1-methyl-4-phenyl-1,2,3,6-tetrahydropyridine (MPTP)-treated nonhuman primates.¹⁶ These lines of evidence suggested that A_{2A} and D_2 receptors play unique and integrative roles in striatal function. A_{2A} antagonists facilitate DA receptor signaling and thereby normalize motor function in animal models of DA dysregulation. As a result of these findings, the adenosine A_{2A} receptor has become a sought after target for treating PD. Blockade of A_{2A} signaling by selective A_{2A} receptor antagonists (e.g., KW-6002,¹⁷ istradefylline; SCH-420814, preladenant¹⁸) was shown to be beneficial for not only enhancing the therapeutic effects of L-DOPA but also reducing dyskinesia from long-term L-DOPA treatment.¹⁹ Preladenant completed phase II clinical trials for PD, and Merck (Schering-Plough) is currently recruiting for several phase III trials.²⁰

Quantitative autoradiographic analyses in rodent, postmortem human brain sections,¹² and [^{11}C -MPDX] PET imaging in human subjects²¹ show that adenosine A_1 receptors are concentrated in neocortex, hippocampus, and striatum. On the basis of anatomical and in vivo microdialysis studies, A_1 receptors appear to be localized presynaptically of DA axon terminals where they inhibit DA release.²² A_1 receptor

antagonists facilitate DA release in the striatum and, like A_{2A} receptors, potentiate DA-mediated responses. Antagonism of both the A_{2A} and the A_1 would be synergistic—inhibition of the A_1 receptor will facilitate DA release, while inhibition of the A_{2A} receptor will enhance postsynaptic responses to DA. Interestingly, the A_1 receptor is also concentrated in neocortical and limbic system structures that are important for cognitive function and has been implicated in antidepressant action. Pharmacological inhibition of A_1 receptors enhances neurotransmitter release in the hippocampus²³ and enhances performance in animal models of learning and memory.²⁴ ASP-5854 is a dual A_{2A}/A_1 antagonist having binding affinities of 1.8 and 9.0 nM for A_{2A} and A_1 , respectively.²⁵ ASP-5854 has shown very good efficacy in a number of animal models of PD,²⁶ and it has shown positive effects in two models of cognition, the scopolamine-induced memory deficits in the mouse Y-maze and the rat passive avoidance test.²⁷ In contrast, the selective A_{2A} antagonist KW-6002 had minimal or no effect in the same models, suggesting that the A_1 component could provide added benefit to PD patients. These data suggest that a dual A_{2A}/A_1 adenosine receptor antagonist may offer a unique and exciting approach to treating both the motor and the nonmotor disturbances of PD.

RESULTS AND DISCUSSION

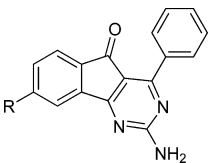
We recently published the in vivo characterization of an arylindenopyrimidine compound **1** as a dual A_{2A}/A_1 receptor antagonist.²⁸ Compound **1** was identified as an ideal dual A_{2A}/A_1 receptor antagonist having excellent functional in vitro activity (A_{2A} $K_i = 4.1$ nM; A_1 $K_i = 17.0$ nM) with good pharmacokinetics (PK) and desirable brain levels. Compound **1** also showed excellent beneficial effects in several preclinical animal models of PD across a number of different species including mouse²⁹ and rat³⁰ models of neuroleptic-induced catalepsy, mouse model of reserpine-induced akinesia,³¹ rat 6-OHDA lesion model of drug-induced rotation,³² and MPTP-treated nonhuman primate model.³³

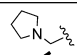
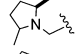
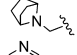
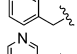
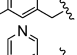
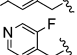
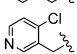
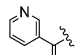
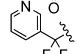
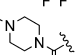
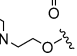
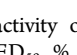
Further evaluation of **1** revealed that it was genotoxic in both the Ames and the mouse lymphoma L5178Y assays following metabolic activation.³⁴ Incubation of **1** with Aroclor 1254-induced rat liver S9 and human liver S9 produced at least two reactive metabolites, the endocyclic iminium ion **2** and the aryl aldehyde **3** (Scheme 1). It was concluded that one of these reactive metabolites was responsible for the genotoxicity based on several mechanistic studies. Compound **1** also showed some adverse events in the 28 day GLP toxicity study in nonhuman primates, which may be related to the reactive metabolites, but that has not been confirmed. Knowing the metabolic soft spots of the molecule allowed us to design analogues that might slow down or eliminate the oxidative metabolism that occurred with compound **1**.

The primary site of metabolism was occurring on the methylenes adjacent to the nitrogen inside the pyrrolidine ring. The addition of methyl groups on one, not shown, or both sides (**4**) of the nitrogen atom gave compounds that were

devoid of the metabolic liability seen with **1**. It appeared that the metabolism was more influenced by the steric bulk of the methyl groups rather than the electronics as one might expect the methine carbons to be more susceptible to oxidation. Also, the methyl groups were able to block metabolism at the benzylic position. The dimethylpyrrolidine **4** maintained good functional (human cell lines) in vitro activity for both A_{2A} and A_1 , but **4** had decreased in vivo activity in the haloperidol-induced catalepsy model in mouse as compared to **1** (Table 1).

Table 1. Human Functional A_{2A} and A_1 in Vitro Activity and Reversal of Neuroleptic-Induced Catalepsy in Mice



Compound	R	A_{2A} cAMP K_i (nM)	A_1 cAMP K_i (nM)	Mouse Catalepsy ^a ED ₅₀ (mg/kg), p.o.
1		4.1	17.0	0.2
4		13.1	37.3	3.2
5		3.1	223	1.0
6		0.3	2.4	<1.0
7		1.4	5.2	100% reversal @ 10 mg/kg
8		1.3	6.0	100% reversal @ 10 mg/kg
9		0.7	2.5	100% reversal @ 10 mg/kg
10		0.1	0.5	100% reversal @ 10 mg/kg
11		0.5	1.8	not active @ 10 mg/kg
12		1.6	29.3	not active @ 10 mg/kg
13		8.2	58.4	0.4
14		6.5	48.2	<0.1

^aThe in vivo activity of reversing haloperidol-induced catalepsy is reported as an ED₅₀, % reversal of at a single dose, or not active at a single dose. Not active corresponds to <50% reversal of catalepsy. Behavioral testing was conducted 1 h after dosing of A_{2A}/A_1 antagonist.

Haloperidol, a neuroleptic medication that inhibits D_2 receptors,³⁵ was used to induce catalepsy. In the rodent, catalepsy is characterized as a loss of voluntary motion where limbs uncharacteristically remain in placed positions, which mimics the muscular stiffness seen in PD patients. Efficacy in this model is defined as reversal of catalepsy, that is, moving from the placed positions (refer to the Experimental Section for a more detailed description of the mouse catalepsy model). This was the primary in vivo model that was used to evaluate compounds quickly by assessing oral and central nervous system activity. Also, the model typically required very little compound (5–10 mg), making it a robust tool with very fast turnaround. The bicyclic pyrrolidine **5** was also devoid of the metabolic liabilities and showed improved in vivo activity with an ED₅₀ of 1 mg/kg in mouse catalepsy, but this was still 5-fold less potent than **1**.

Next, we replaced the benzylic pyrrolidine with various substituted pyridine compounds exemplified by **6–12**. The thought was to remove the electron-rich ring with the pyridine, a system that would still increase solubility. Compounds **6–10** had very potent activity for A_{2A} and A_1 , while maintaining excellent activity in the mouse catalepsy model. A dose response was run using **6** in the mouse catalepsy model and showed that it had an ED₅₀ of <1 mg/kg after oral administration. Not surprisingly, the benzylic pyridines were extensively metabolized at the benzylic position, which resulted in poor plasma exposures and very short half-lives (<0.5 h). The behavioral testing was generally conducted 1 h after dosing the A_{2A}/A_1 antagonist, but a duration of action study showed that **6** and **7** were active in the mouse catalepsy model at 4 and 2 h, respectively, after a 10 mg/kg po dose despite the very short half-life. The suboptimal PK profiles and benzylic metabolism prompted us to prepare the ketone **11** and the *gem*-difluoro **12** to try and block metabolism, improve stability, and increase in vivo exposure. The metabolism was eliminated, and the compounds maintained good in vitro activity, but neither **11** or **12** was active in the mouse catalepsy model after a 10 mg/kg oral dose. Although no PK or brain levels were determined for **11** or **12**, the poor physical properties, that is, solubility, may be responsible for low absorption and lack of activity. Moving the pyridine ring out by one or two methylenes results in decreased in vitro activity.

Converting the benzyl amines to their corresponding amides gave compounds with excellent in vitro and in vivo activity.^{28c} Compound **13** is a representative compound from the amide series that had optimal potency (ED₅₀ = 0.4 mg/kg) in the mouse catalepsy model as compared to other amides that were prepared (Figure 1). Cyclic amines generally gave amide compounds that were slightly more potent than acyclic amines. The idea behind preparing the amides was 2-fold: first, oxidizing the benzylic position would eliminate the oxidative metabolism at that position; second, the electron-withdrawing nature of the carbonyl would pull electron density out of the nitrogen heterocycle, making the positions α to the nitrogen less susceptible to oxidation. Introduction of a basic nitrogen, like the one found in the piperazine, was critical to maintain good solubility. Fortunately, this approach was successful as we observed no metabolism on the methylenes adjacent to the nitrogen of the amide nor did we see any metabolism on the methylenes adjacent to the nitrogen in the 4-position.

Another strategy to eliminate the benzylic metabolism was to prepare a variety of phenyl ethers from this series.^{28c} Converting the benzylic methylene to an oxygen atom eliminated the metabolic potential at that position, similarly to the carbonyl from the amides. Moving the solubilizing group, nitrogen heterocycle, out a few atoms also eliminated the oxidative metabolism from occurring inside the ring as seen with compound **1**, while maintaining good activity. Compound **14** represents the optimized compound out of a variety of ethers that were synthesized. The morpholine ring gave optimal in vitro and in vivo activity and had an ED₅₀ of <0.1 mg/kg in the mouse catalepsy model (Figure 1).

Chemistry. The synthesis of compounds **4–13** started with the commercially available 6-methylindanone **15**, which was deprotonated with NaHMDS and reacted with CS₂ followed by MeI to afford the dithioketenacetal **16** (Scheme 2).^{28,36} Compound **16** reacts with guanidine to form an intermediate amino pyrimidine, not shown, that is then oxidized to the corresponding ketone by passing air through the solution to

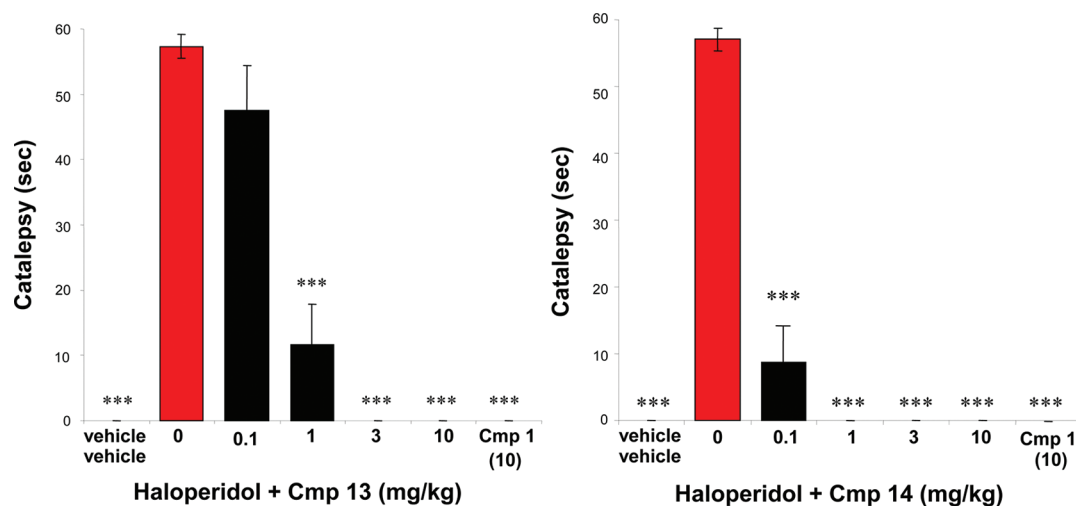


Figure 1. Reversal of neuroleptic-induced catalepsy in mice by compounds 13 and 14. In this behavioral model, catalepsy was induced in male Balb/c mice by subcutaneous administration of haloperidol, a neuroleptic D₂ receptor antagonist. Compound 1 was used as the positive control for this model at 10 mg/kg, po. Compounds 13 (left panel) and 14 (right panel) were administered orally 30 min after haloperidol (1 mg/kg, sc). Behavioral testing was conducted 1 h after dosing of 13 and 14. Each value represents average (\pm SEM) time in cataleptic position of $n = 8$ –12 mice per treatment group during a 60 s test session. Both compounds produced a dose-dependent reversal of haloperidol-induced catalepsy. The ED₅₀ of 13 for inhibiting haloperidol-induced catalepsy in mice was 0.4 mg/kg, po, and the minimum effective dose is shown to be 1 mg/kg, po. The ED₅₀ of 14 for inhibiting haloperidol-induced catalepsy in mice was <0.1 mg/kg, po, and the minimum effective dose is shown to be 0.1 mg/kg, po. Asterisks indicate significant differences as compared with the haloperidol + vehicle control treatment group ($***P < 0.001$, Dunnett's test of multiple comparisons).

give 17.³⁷ The amino pyrimidine was protected using excess (Boc)₂O and 4-(dimethylamino)pyridine (DMAP) to give 18. Efforts to mono-Boc compound 17 were unsuccessful as the di-Boc compound was forming while starting material was present. Also, the reaction was very sluggish without the addition of DMAP. The phenyl substituent was installed via a modified Suzuki reaction under Liebeskind type conditions using the methylthioether as the coupling partner to afford 19.³⁸ The Suzuki reaction proceeded smoothly with the di-Boc protected amino pyrimidine but could not be accomplished on the unprotected amino pyrimidine 17 under the same conditions. Compound 19 underwent benzyl bromination to afford the corresponding bromide 20, which was a key intermediate that was carried through paths 1–3 to prepare compounds 4–13. Following path 1, the Boc groups were removed with TFA followed by alkylation with 2,5-dimethylpyrrolidine or 7-azabicyclo[2.2.1]heptane to give the desired target compounds 4 and 5, respectively. Following path 2, the benzyl bromide 20 was reacted, under Suzuki conditions, with several pyridylboronic acids to provide their corresponding compounds 6–10. The pyridyl compound 6 was oxidized using air, under basic conditions in NMP, to give the diketone 11 (see insert Scheme 2). Reaction of 11 with DAST gave the *gem*-difluoro compound 12. Following path 3, the bromide 20 was converted to the corresponding aldehyde, not shown, using NMO in the presence of molecular sieves followed by further oxidation to the acid 21 with KMnO₄. The acid 21 was coupled with 1-methylpiperazine using HATU followed by removal of the Boc groups with TFA afforded the amide 13.

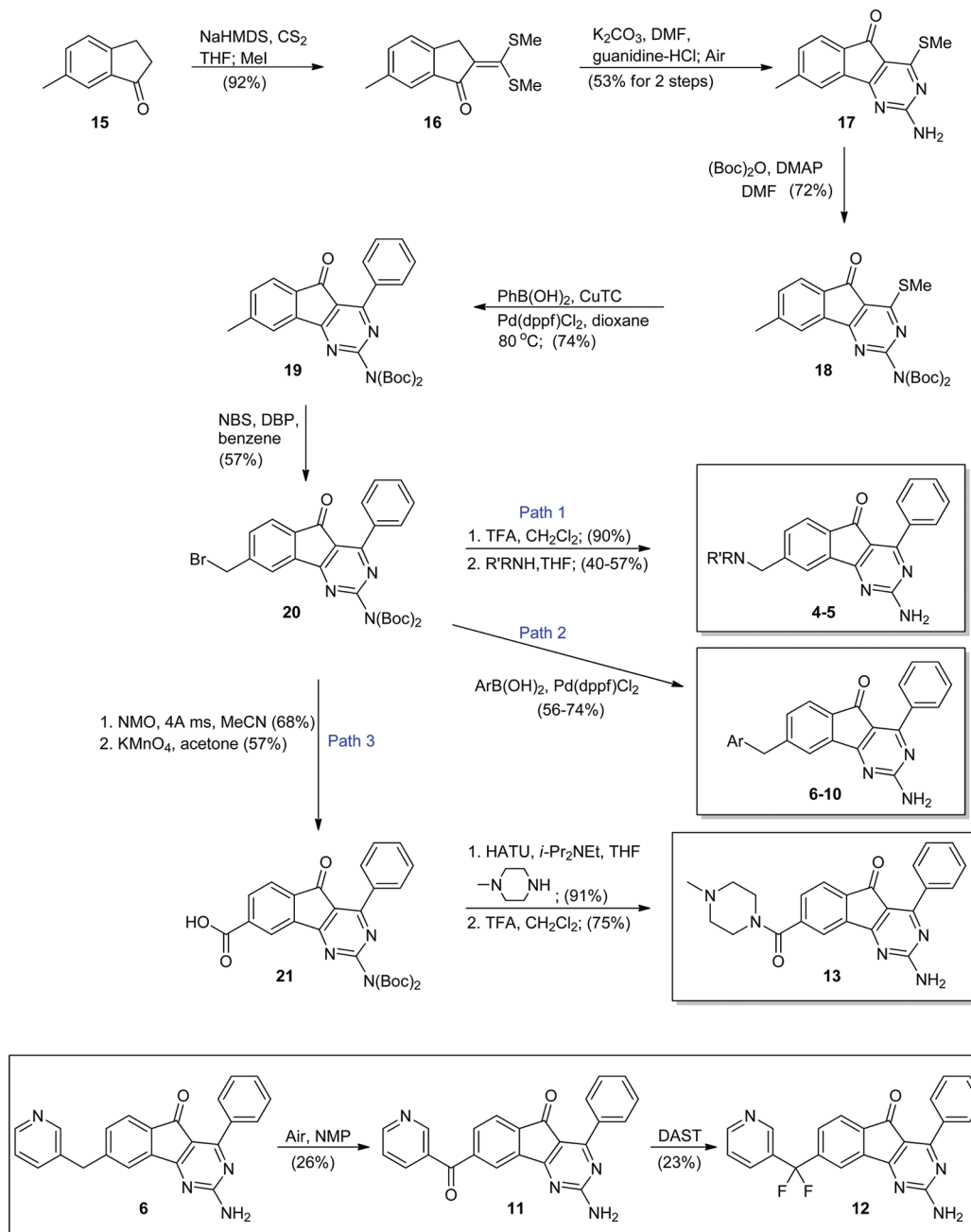
The synthesis of 14 started with the commercially available 6-methoxyindanone 22, which was condensed with benzaldehyde to afford the benzylidene 23 (Scheme 3).²⁸ The benzylidene 23 was reacted with guanidine and, upon aromatization, was oxidized to the corresponding ketone 24 using air in a one-pot reaction as described above.³⁷ The methoxy group was deprotected by LiCl in NMP at 180 °C to

give the corresponding phenol 25. Attempts to deprotect using BBr₃ were completely unsuccessful. However, EtSn₄ in DMF was also effective in removing the methoxy group but was not as efficient as the LiCl. The phenol was then reacted with 4-(2-chloroethyl)morpholine in the presence of *t*-BuOK to give the ether 14.

PK. Compounds 13 and 14 were of high interest because of their *in vivo* potency in the mouse catalepsy model, shown above, and because of their different structural features. The PK data of 13 and 14 were determined in mouse, rat, and monkey and compared to the PK data of 1 (Table 2). Compounds 1, 13, and 14 had moderate to high clearances in all species. In general, the compounds had good oral bioavailability and low to moderate half-lives in all species. Amide 13 had half-lives 2–4-fold higher in rodents as compared to compounds 1 and 14. Plasma levels of 13 and 14 were good in all species and were comparable to 1 in mouse and rat but were 2–4-fold higher in monkeys as compared to 1. The concentration of 14 found in rat brain (4161 nM) was comparable to the brain concentration (3552 nM) found using compound 1. Interestingly, 13 had a much lower exposure in the brain (459 nM) but showed similar efficacy in the mouse catalepsy model as compared to 1 (Table 1). The different brain exposures of 13 and 14 were compelling, and we thought that further characterization of both compounds would complement one another. Our goal was to profile both compounds to get a better understanding of what may be the ideal brain exposure and PK profile for a dual adenosine A_{2A}/A₁ antagonist for the treatment of PD.

Mouse Catalepsy. The mouse catalepsy data,²⁹ Figure 1, were collected at a single time point, 1 h postdose of 13 or 14. Another study was performed using the same model of neuroleptic-induced catalepsy in mice to examine the duration of action of 13 and 14.³⁵ Catalepsy time was measured in haloperidol (1 mg/kg, sc)-treated mice after oral administration of 13 (10 mg/kg), 14 (10 mg/kg), vehicle, or positive control 1 (10 mg/kg). Catalepsy was measured at 30 min and 1, 2, and 4

Scheme 2. Synthesis of Compounds 4–13



h after oral dosing of the respective treatment groups. The results in Figures 2 and 3 show that haloperidol induced catalepsy at each measurement period and that 13 and 14 were effective in reversing haloperidol-induced catalepsy at all measurement periods. These data suggest that in mice, the duration of action for in vivo efficacy of 13 and 14 is at least 4 h following oral administration at 10 mg/kg. Extended measurement periods past 4 h were not examined nor were lower doses of compounds 13 or 14.

Rat Catalepsy. In vivo efficacy of 13 and 14 was examined in a rat model of neuroleptic-induced catalepsy.³⁰ This model was carried out analogously to that described for mice except that the maximum duration for rat was 180 s as compared to 60 s for mice. Results in Figure 4 show that both 13 and 14 were effective in reversing the haloperidol-induced catalepsy having ED₅₀ values of 0.6 and 0.3 mg/kg, po, respectively, and each

having minimum effective doses of 1 mg/kg, po. As shown in mice, the reversal in rat was also dose-dependent.

A study was performed using the rat model of neuroleptic-induced catalepsy to examine the duration of action of 14. The results in Figure 5 shows that haloperidol induced catalepsy at each measurement period and that 14 was effective in reversing haloperidol-induced catalepsy at 1, 2, and 4 h after a 1 mg/kg oral dose. Positive results were also observed for 1 (positive control) at 10 mg/kg, po. These data suggest that in rats, the duration of action for in vivo efficacy of 14 is at least 4 h following oral administration.

Mouse and Rat Models of Reserpine-Induced Akinesia. To evaluate the potential antiparkinsonian properties of 13 and 14, locomotor activity was studied in a mouse model of reserpine-induced akinesia.^{31,39} Reserpine is an alkaloid that depletes monoamine by inhibiting its vesicular uptake, resulting

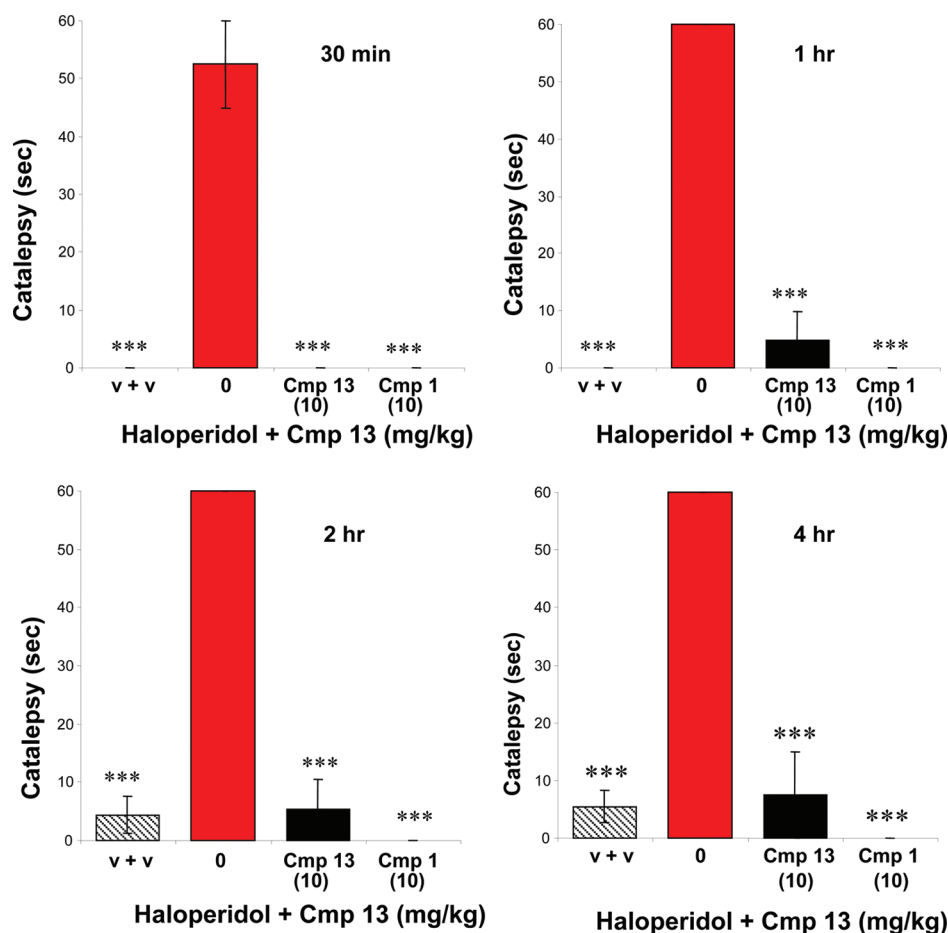


Figure 2. Duration of action of 13 in the mouse model of neuroleptic-induced catalepsy. Catalepsy was induced by subcutaneous administration of haloperidol. Compound 13 was administered orally 30 min after haloperidol (1 mg/kg, sc). Behavioral testing was conducted 30 min and 1, 2, and 4 h after administration of vehicle, 13, or 1 (positive control) in male Balb/c mice. Each value represents average (\pm SEM) time in cataleptic position of $n = 8$ mice per treatment group during a 60 s test session. Haloperidol-induced catalepsy was evident at all measurement periods. Compound 13 was effective in reversing haloperidol-induced catalepsy 30 min and 1, 2, and 4 h after oral dosing. Asterisks indicate significant differences as compared with the haloperidol + vehicle control treatment group ($***P < 0.001$, Dunnett's test of multiple comparisons).

known that approximately 80% of DA neurons are depleted before any PD symptoms, that is, motor dysfunction, is apparent.⁴¹ Therefore, it is critical to identify PD patients at an earlier stage to maximize the benefit of adenosine receptor antagonists in treating PD. While this remains the ultimate challenge, significant efforts are being put forth to evaluate and treat PD patients to enhance quality of life.

In summary, we have shown that the dual A_{2A}/A_1 receptor antagonist **1** was metabolized into reactive intermediates that caused genotoxicity and possibly the adverse events seen in the 28 day GLP toxicity study in nonhuman primates. Optimization of the scaffold led to the identification of **13** and **14** as dual A_{2A}/A_1 receptor antagonists having complementary brain PK profiles. Both **13** and **14** showed excellent efficacy across a number of animal models of PD including mouse and rat catalepsy, mouse and rat reserpine-induced akinesia, and 6-OHDA lesion model in rats. Despite the fact that **14** had ~8-fold higher brain levels in rats as compared to **13**, both **13** and **14** exhibit very similar efficacy profiles across the various PD models. Further evaluation will be needed to differentiate or distinguish compounds **13** and **14**.

EXPERIMENTAL SECTION

General Information. All proton and carbon nuclear magnetic resonance spectra were determined using a 400 MHz Bruker NMR with the appropriate internal standards. High-resolution MS was performed on a JEOL Accutof JMS-T100 LC with a DART CE ionization source operating in the positive mode. Reagent grade chemicals and solvents were purchased from Aldrich, Oakwood, or TCI. All chromatographies were carried out on a combi-flash system equipped with an automated fraction collector. All final compounds were purified to $\geq 95\%$ purity as determined by Agilent 1100 series high-performance liquid chromatography (HPLC) with UV detection at 254 nm using the following method: Supelcosil ABZ+PLUS, 3.3 cm \times 2.1 cm, 11 min; 1.2 mL/min flow rate; and 5–95% 0.1% TFA in $CH_3CN/0.1\%$ TFA in H_2O . Experimental procedures and spectral listings for compounds **1** and **16–20** were previously reported.^{28a}

2-Amino-8-((2,5-dimethylpyrrolidin-1-yl)methyl)-4-phenyl-5H-indeno[1,2-d]pyrimidin-5-one (4). Neat TFA (8 mL, 102.8 mmol) was added to a CH_2Cl_2 solution (24 mL) of **20** (1.94 g, 3.4 mmol), and the mixture was stirred at room temperature. After 2 h, the solution was concentrated in vacuo, and saturated aqueous $NaHCO_3$ was added to the material. The resulting suspension was sonicated, and the precipitate was collected by filtration and washed with water. The collected solid was dried under high vacuum to afford 1.1 g (90%) of 2-amino-8-(bromomethyl)-4-phenyl-5H-indeno[1,2-d]pyrimidin-5-one as a yellow solid that was used without further purification. $R_t = 4.75$ min. 1H NMR (400 MHz, chloroform- d): δ 8.03–8.12 (m, 2H),

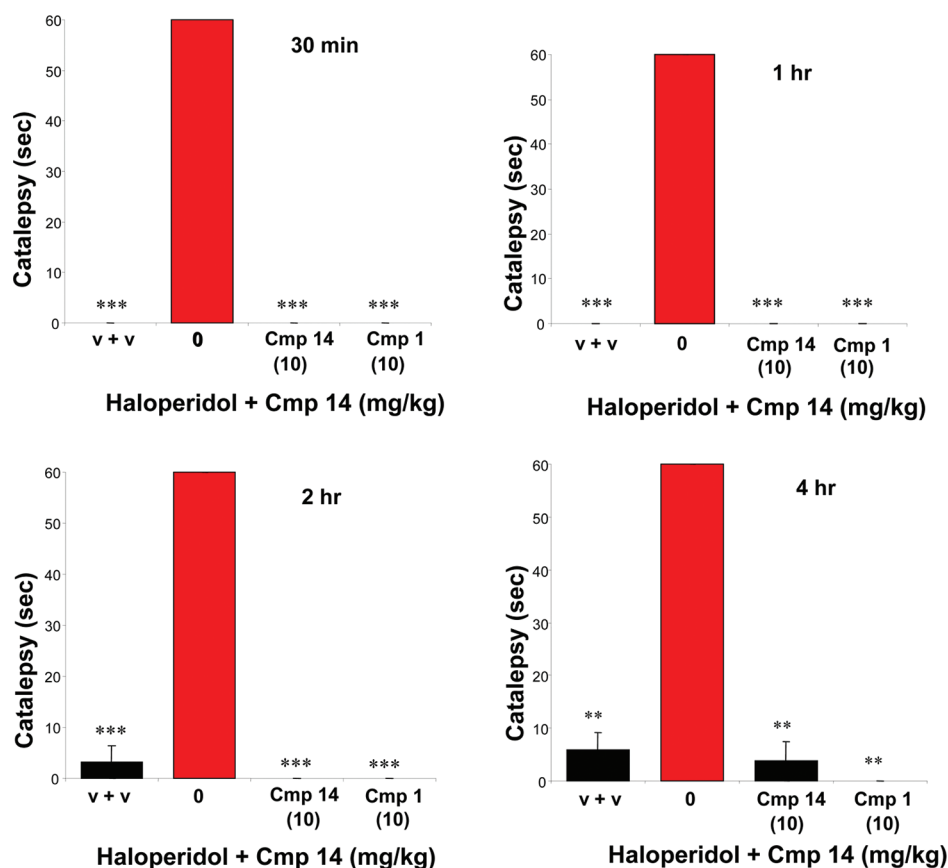


Figure 3. Duration of action of 14 in the mouse model of neuroleptic-induced catalepsy. Catalepsy was induced by subcutaneous administration of haloperidol. Compound 14 was administered orally 30 min after haloperidol (1 mg/kg, sc). Behavioral testing was conducted 30 min and 1, 2, and 4 h after administration of vehicle, 14, or 1 (positive control) in male Balb/c mice. Each value represents average (\pm SEM) time in cataleptic position of $n = 8$ mice per treatment group during a 60 s test session. Haloperidol-induced catalepsy was evident at all measurement periods. Compound 14 was effective in reversing haloperidol-induced catalepsy 30 min and 1, 2, and 4 h after oral dosing. Asterisks indicate significant differences as compared with the haloperidol + vehicle control treatment group ($***P < 0.001$, Dunnett's test of multiple comparisons).

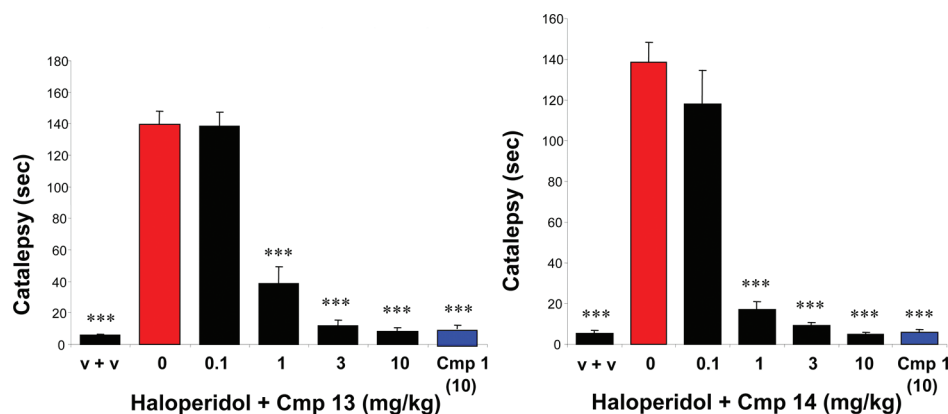


Figure 4. Reversal of neuroleptic-induced catalepsy in rats by compounds 13 and 14. In this behavioral model, catalepsy was induced in Sprague–Dawley rats by subcutaneous administration of haloperidol, a neuroleptic D_2 receptor antagonist. Compound 1 was used as the positive control for this model at 10 mg/kg, po. Compounds 13 (left panel) and 14 (right panel) were administered orally 60 min after haloperidol (1 mg/kg, sc). Behavioral testing was conducted 1 h after dosing of 13 and 14. Each value represents average (\pm SEM) time in cataleptic position of $n = 10$ rats per treatment group during a 180 s test session. Both compounds produced a dose-dependent reversal of haloperidol-induced catalepsy. The ED_{50} values of 13 and 14 for inhibiting haloperidol-induced catalepsy in rats were 0.6 and 0.3 mg/kg, po, respectively, and the minimum effective dose was shown to be 1 mg/kg, po, for both 13 and 14. Asterisks indicate significant differences as compared with the haloperidol + vehicle control treatment group ($***P < 0.001$, Dunnett's test of multiple comparisons).

7.89 (d, $J = 0.98$ Hz, 1H), 7.72 (d, $J = 7.58$ Hz, 1H), 7.46–7.62 (m, 4H), 5.88 (br. s., 2H), 4.56 (s, 2H) ppm. ^{13}C NMR (101 MHz, chloroform- d): δ 187.6, 176.1, 165.9, 164.5, 144.2, 140.6, 136.4, 135.2,

133.4, 131.4, 129.7, 128.1, 124.0, 122.0, 108.0, 32.1 ppm. HRMS, m/z calcd for $C_{18}H_{13}BrN_3O [(M + H)^+]$, 366.0237; found, 366.0254.

Neat 2,5-dimethylpyrrolidine-mix of *cis*- and *trans*-isomers (1.1 mL, 9.3 mmol) was added to a THF solution (20 mL) of 2-amino-8-

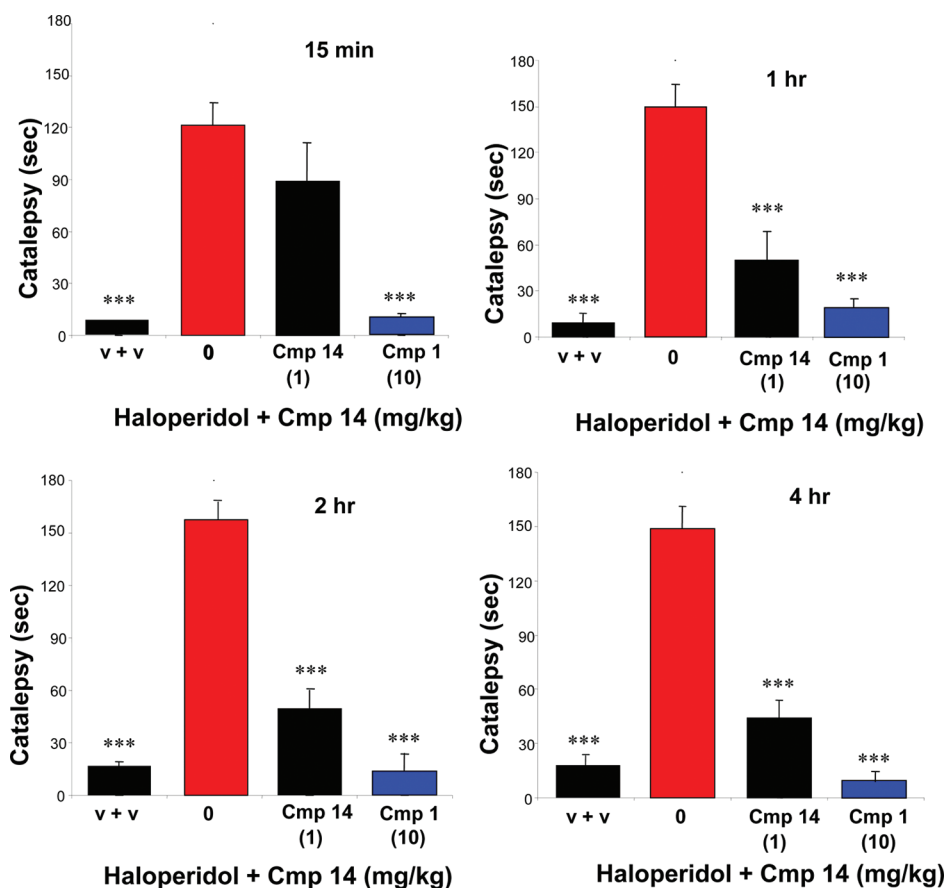


Figure 5. Duration of action of 14 in the rat model of neuroleptic-induced catalepsy. Catalepsy was induced by subcutaneous administration of haloperidol. Compound 14 (1 mg/kg) was administered orally 60 min after haloperidol (1 mg/kg, sc). Behavioral testing was conducted 15 min and 1, 2, and 4 h after administration of vehicle, 14, or 1 (positive control) in Sprague–Dawley rats. Each value represents average (\pm SEM) time in cataleptic position of $n = 10$ –12 rats per treatment group during a 180 s test session. Haloperidol-induced catalepsy was evident at all measurement periods. Compound 14 was effective in reversing haloperidol-induced catalepsy 1, 2, and 4 h after oral dosing of 1 mg/kg. Asterisks indicate significant differences as compared with the haloperidol + vehicle control treatment group (** $P < 0.001$, Dunnett's test of multiple comparisons).

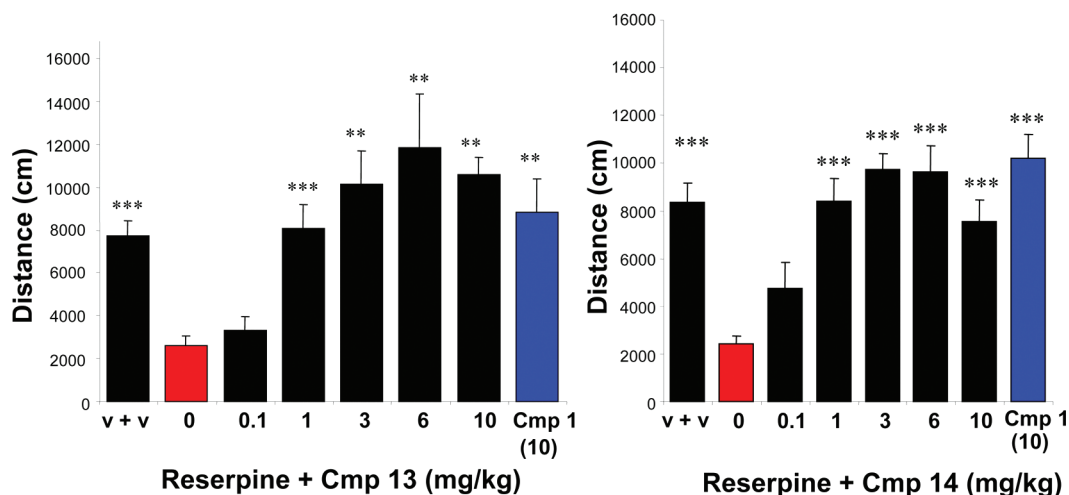


Figure 6. Reversal of reserpine-induced akinesia by 13 (left) and 14 (right) in mice. In this behavioral model, akinesia was induced by subcutaneous administration reserpine, a monoamine-depleting drug in male CF-1 mice. Compounds 13, 14, 1 (10 mg/kg, positive control), or vehicle were administered orally 60 min before the behavioral test in the locomotor activity boxes. Each value shows the mean (\pm SEM) of the total distance traveled during the 30 min measurement period in the behavioral test session. Reserpine produced a marked decrease in locomotor activity as compared with vehicle + vehicle-treated controls. Compounds 13 and 14 reversed reserpine-induced akinesia with similar effectiveness to the control 1, $N = 14$ –16 mice per treatment group. Asterisks indicate significant differences as compared with the reserpine + vehicle control group (** $P < 0.01$, *** $P < 0.001$, Hochberg test of multiple comparisons).

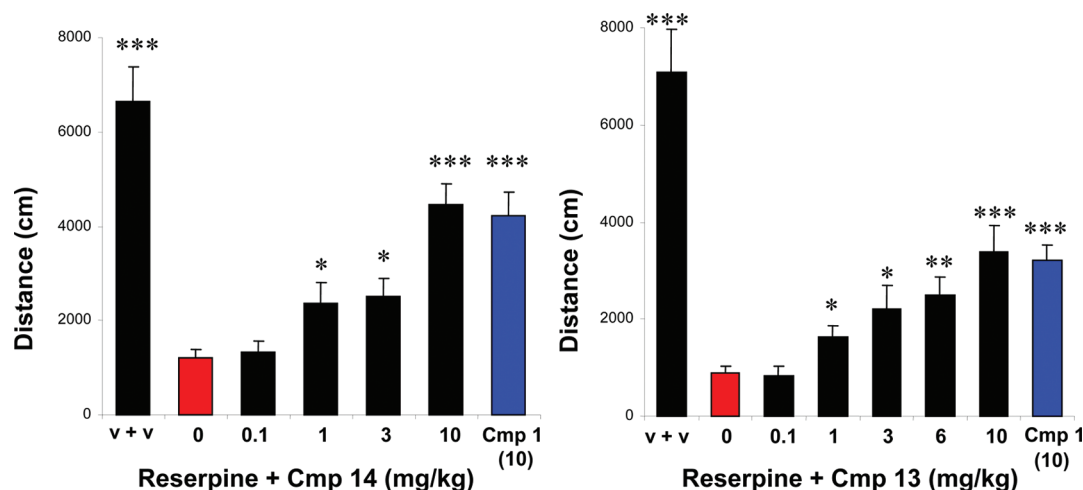


Figure 7. Reversal of reserpine-induced akinesia by 14 (left) and 13 (right) in rats. In this behavioral model, akinesia was induced by subcutaneous administration reserpine, a monoamine-depleting drug in male Wistar rats. Compounds 13, 14, 1 (10 mg/kg, positive control), or vehicle was administered orally 60 min before the behavioral test in the locomotor activity boxes. Each value shows the mean (\pm SEM) of the total distance traveled during a 60 min measurement period in the behavioral test session. Reserpine produced a marked decrease in locomotor activity as compared with vehicle + vehicle-treated controls. Compounds 13 and 14 reversed reserpine-induced akinesia with similar effectiveness to the control 1, $N = 16$ –18 rats per treatment group. Asterisks indicate significant differences as compared with the reserpine + vehicle control group (* $P < 0.05$, ** $P < 0.01$, and *** $P < 0.001$, Hochberg test of multiple comparisons).

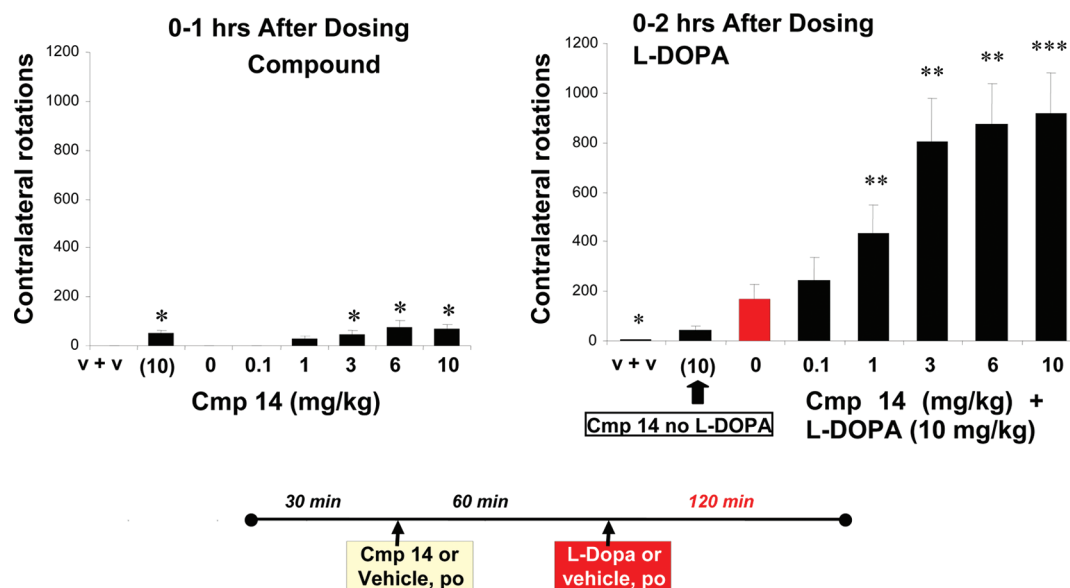


Figure 8. Compound 14 potentiates the effects of L-DOPA in the 6-OHDA-lesioned rat model of PD. Six weeks after administration of 6-OHDA, the behavioral test was started by dosing rats with L-DOPA [10 mg/kg, po coadministered with carbidopa (2.5 mg/kg, sc)] alone or with each dose of 14 (0.1, 1.0, 3.0, 6.0, and 10 mg/kg, po). The effects of 14 alone at 10 mg/kg, po (indicated in both the left and the right panels at 10), were also studied in this model. For clarity, two separate groups of animals were dosed at 10 mg/kg, po. The rotational behavior was determined as each animal was tethered to a high-resolution optical sensor connected to an automated computerized system that quantifies circular motion. One rotation count was defined as one 360° turn. Each value represents the mean (\pm SEM) of total contralateral rotations of $n = 16$ rats per treatment group during the 2 h before and after L-DOPA administration. Asterisks in the left panel indicate significant differences as compared with vehicle control treatment group, and asterisks in the right panel indicate significant differences as compared with the L-DOPA + vehicle control treatment group (* $P < 0.05$, ** $P < 0.01$, and *** $P < 0.001$, Tukey's test of multiple comparisons).

(bromomethyl)-4-phenyl-5H-indeno[1,2-*d*]pyrimidin-5-one (1.7 g, 4.6 mmol) and triethyl amine (Et_3N) (1.3 mL, 9.3 mmol), and the resulting mixture was heated to 75°C . After 3 h, the mixture was concentrated in vacuo, dissolved into CH_2Cl_2 . The mixture was washed with saturated aqueous NaHCO_3 and brine (2 \times), dried (Na_2SO_4), concentrated, and purified via column chromatography to give 1.0 g (57%) of 4. Compound 4 was dissolved in CH_2Cl_2 and added dropwise to an excess of HCl in ether. The resulting precipitate was filtered off to give 1.1 g of 2-amino-8-((2,5-dimethylpyrrolidin-1-yl)methyl)-4-phenyl-5H-indeno[1,2-*d*]pyrimidin-5-one (4) as the di-

HCl salt. $R_t = 5.57$ min. ^1H NMR (400 MHz, $\text{DMSO-}d_6$): δ 8.12 (d, $J = 9.60$ Hz, 1H), 8.01 (d, $J = 8.59$ Hz, 4H), 7.87 (d, $J = 7.58$ Hz, 1H), 7.72–7.80 (m, 1H), 7.45–7.62 (m, 4H), 4.58 (d, $J = 4.55$ Hz, 2H), 3.45–3.55 (m, 2H), 2.07–2.24 (m, 2H), 1.59–1.75 (m, 2H), 1.34 (s, 3H), 1.33 (s, 3H) ppm. ^{13}C NMR (101 MHz, $\text{DMSO-}d_6$): δ 186.6, 175.2, 165.1, 164.8, 139.7, 136.9, 136.2, 136.1, 135.5, 130.9, 129.4, 127.6, 123.8, 123.2, 110.9, 63.1, 52.6, 29.3, 16.4 ppm. HRMS, m/z calcd for $\text{C}_{24}\text{H}_{25}\text{N}_4\text{O}$ [($\text{M} + \text{H}$) $^+$], 385.2023; found, 385.2036.

8-(7-Azabicyclo[2.2.1]heptan-7-ylmethyl)-2-amino-4-phenyl-5H-indeno[1,2-*d*]pyrimidin-5-one (5). The same procedure described to

prepare **4** was followed except that 7-azabicyclo[2.2.1]heptane was used in place of 2,5-dimethylpyrrolidine to give the title compound in 40% yield. $R_t = 3.04$ min. $^1\text{H NMR}$ (400 MHz, DMSO- d_6): δ 8.05–8.16 (m, 3H), 8.01 (d, $J = 7.07$ Hz, 2H), 7.97 (d, $J = 7.58$ Hz, 1H), 7.75 (d, $J = 7.58$ Hz, 1H), 7.48–7.61 (m, 3H), 4.38 (d, $J = 6.06$ Hz, 2H), 3.95 (br. s., 2H), 2.24 (d, $J = 8.59$ Hz, 2H), 2.04 (d, $J = 8.59$ Hz, 2H), 1.77 (d, $J = 8.59$ Hz, 2H), 1.67 (d, $J = 8.08$ Hz, 2H) ppm. $^{13}\text{C NMR}$ (101 MHz, DMSO- d_6): δ 186.8, 175.4, 164.8, 164.7, 139.9, 137.7, 136.8, 135.4, 135.3, 131.0, 129.5, 127.7, 123.3, 123.2, 111.0, 62.7, 48.3, 26.9, 25.1 ppm. HRMS, m/z calcd for $\text{C}_{24}\text{H}_{23}\text{N}_4\text{O}$ [(M + H) $^+$], 383.1866; found, 383.1848.

2-Amino-4-phenyl-8-(pyridin-3-ylmethyl)-5H-indeno[1,2-d]pyrimidin-5-one (6). A dioxane/water (4:1) solution (5 mL) of 2-amino-8-(bromomethyl)-4-phenyl-5H-indeno[1,2-d]pyrimidin-5-one (175 mg, 0.48 mmol), 3-pyridylboronic acid (94 mg, 0.77 mmol), K_2CO_3 (133 mg, 0.96 mmol), and Pd(dppf) Cl_2 (39 mg, 0.05 mmol) was heated in the microwave at 120 °C for 10 min. The resulting mixture was diluted with THF and EtOAc, washed with water and brine, dried (Na_2SO_4), concentrated, and purified to give 112 mg (64%) of **6**. Compound **6** was dissolved in THF added dropwise to an excess of HCl in ether. The resulting precipitate was filtered off to give 115 mg of 2-amino-4-phenyl-8-(pyridin-3-ylmethyl)-5H-indeno[1,2-d]pyrimidin-5-one (**6**) as the di-HCl salt. $R_t = 3.01$ min. $^1\text{H NMR}$ (400 MHz, DMSO- d_6): δ 9.01 (s, 1H), 8.84 (d, $J = 5.05$ Hz, 1H), 8.54 (d, $J = 8.08$ Hz, 1H), 7.91–8.12 (m, 5H), 7.73 (s, 1H), 7.65 (s, 2H), 7.46–7.59 (m, 3H), 4.39 (s, 2H) ppm. $^{13}\text{C NMR}$ (101 MHz, DMSO- d_6): δ 186.9, 175.4, 164.6, 164.3, 145.9, 145.7, 141.7, 140.3, 140.1, 135.3, 135.2, 134.9, 133.5, 130.8, 129.4, 127.6, 127.0, 123.5, 121.4, 111.0, 37.1 ppm. HRMS, m/z calcd for $\text{C}_{23}\text{H}_{17}\text{N}_4\text{O}$ [(M + H) $^+$], 365.1379; found, 365.1395.

5-((2-Amino-5-oxo-4-phenyl-5H-indeno[1,2-d]pyrimidin-8-yl)methyl)nicotinonitrile (7). The same procedure used to prepare **6** was followed except that (5-cyanopyridin-3-yl)boronic acid was used in place of 3-pyridylboronic acid to give the title compound in 64% yield. $R_t = 4.33$ min. $^1\text{H NMR}$ (400 MHz, DMSO- d_6): δ 8.86–8.97 (m, 2H), 8.34 (s, 1H), 7.99 (d, $J = 7.07$ Hz, 3H), 7.45–7.70 (m, 7H), 4.25 (s, 2H) ppm. $^{13}\text{C NMR}$ (101 MHz, DMSO- d_6): δ 186.9, 175.4, 164.5, 164.2, 153.6, 150.4, 146.4, 140.0, 139.9, 136.5, 135.2, 134.7, 133.4, 130.8, 129.4, 127.6, 123.4, 121.2, 116.8, 111.0, 109.0, 37.3 ppm. HRMS, m/z calcd for $\text{C}_{24}\text{H}_{16}\text{N}_5\text{O}$ [(M + H) $^+$], 390.1349; found, 390.1395.

2-Amino-8-((5-fluoropyridin-3-yl)methyl)-4-phenyl-5H-indeno[1,2-d]pyrimidin-5-one (8). The same procedure used to prepare **6** was followed except that (5-fluoropyridin-3-yl)boronic acid was used in place of 3-pyridylboronic acid to give the title compound in 74% yield. $R_t = 3.92$ min. $^1\text{H NMR}$ (400 MHz, DMSO- d_6): δ 8.62 (d, $J = 6.06$ Hz, 2H), 8.20 (br. s., 2H), 7.91–8.03 (m, 3H), 7.69 (s, 1H), 7.62–7.68 (m, 2H), 7.45–7.61 (m, 3H), 4.27 (s, 2H) ppm. HRMS, m/z calcd for $\text{C}_{23}\text{H}_{16}\text{FN}_4\text{O}$ [(M + H) $^+$], 383.1303; found, 383.1229.

2-Amino-8-((3-fluoropyridin-4-yl)methyl)-4-phenyl-5H-indeno[1,2-d]pyrimidin-5-one (9). The same procedure used to prepare **6** was followed except that (3-fluoropyridin-4-yl)boronic acid was used in place of 3-pyridylboronic acid to give the title compound in 69% yield. $R_t = 3.63$ min. $^1\text{H NMR}$ (400 MHz, DMSO- d_6): δ 8.66 (s, 1H), 8.48 (d, $J = 4.04$ Hz, 1H), 8.02–8.15 (br. s., 2H), 7.99 (d, $J = 7.07$ Hz, 2H), 7.44–7.71 (m, 7H), 4.28 (s, 2H) ppm. $^{13}\text{C NMR}$ (101 MHz, DMSO- d_6): δ 186.9, 175.4, 164.6, 164.3, 145.2, 144.8, 142.5, 140.0, 136.6, 135.3, 135.0, 133.4, 130.9, 129.5, 127.7, 126.4, 123.5, 121.0, 119.7, 111.0, 33.7 ppm. HRMS, m/z calcd for $\text{C}_{23}\text{H}_{16}\text{FN}_4\text{O}$ [(M + H) $^+$], 383.1303; found, 383.1322.

2-Amino-8-((4-chloropyridin-3-yl)methyl)-4-phenyl-5H-indeno[1,2-d]pyrimidin-5-one (10). The same procedure used to prepare **6** was followed except that (4-chloropyridin-3-yl)boronic acid was used in place of 3-pyridylboronic acid to give the title compound in 56% yield. $R_t = 3.60$ min. $^1\text{H NMR}$ (400 MHz, DMSO- d_6): δ 8.99 (s, 1H), 8.73 (d, $J = 5.56$ Hz, 1H), 8.15 (br. s., 2H), 7.90–8.03 (m, 3H), 7.45–7.68 (m, 6H), 4.40 (s, 2H) ppm. $^{13}\text{C NMR}$ (101 MHz, DMSO- d_6): δ 186.7, 175.4, 164.2, 164.1, 147.5, 145.3, 144.6, 139.8, 134.9, 135.7, 134.7, 134.7, 133.6, 131.0, 129.5, 127.7, 126.5, 123.4, 121.0, 111.0, 35.7

ppm. HRMS, m/z calcd for $\text{C}_{23}\text{H}_{16}\text{ClN}_4\text{O}$ [(M + H) $^+$], 399.1007; found, 399.1013.

2-Amino-8-nicotinoyl-4-phenyl-5H-indeno[1,2-d]pyrimidin-5-one (11). Powdered NaOH (420 mg, 10.5 mmol) was added to an NMP solution (1.5 mL) of 2-amino-4-phenyl-8-(pyridin-3-ylmethyl)-5H-indeno[1,2-d]pyrimidin-5-one (**6**) (400 mg, 1.1 mmol). Air was bubbled into the solution at a steady rate using a steel needle, and the mixture was heated to 80 °C. After 18 h, the air needle was removed, and water was added. The resulting solid was filtered off, washed with water, and dried in vacuo. The crude solid was dissolved in THF and dry packed onto silica gel. Column chromatography gave 110 mg (26%) of 2-amino-8-nicotinoyl-4-phenyl-5H-indeno[1,2-d]pyrimidin-5-one (**11**). $R_t = 3.56$ min. $^1\text{H NMR}$ (400 MHz, DMSO- d_6): δ 8.97 (s, 1H), 8.89 (d, $J = 4.55$ Hz, 1H), 8.13–8.25 (m, 3H), 8.00–8.10 (m, 4H), 7.86 (d, $J = 7.58$ Hz, 1H), 7.66 (dd, $J = 5.31, 7.83$ Hz, 1H), 7.48–7.61 (m, 3H) ppm. $^{13}\text{C NMR}$ (151 MHz, DMSO- d_6): δ 194.1, 186.9, 175.4, 165.9, 165.5, 153.7, 150.6, 141.4, 140.1, 140.0, 137.7, 136.0, 135.2, 132.9, 131.6, 130.0, 128.3, 124.3, 123.9, 122.0, 111.7 ppm. HRMS, m/z calcd for $\text{C}_{23}\text{H}_{15}\text{N}_4\text{O}_2$ [(M + H) $^+$], 379.1190; found, 379.1221.

2-Amino-8-(difluoro(pyridin-3-yl)methyl)-4-phenyl-5H-indeno[1,2-d]pyrimidin-5-one (12). 2-Amino-8-nicotinoyl-4-phenyl-5H-indeno[1,2-d]pyrimidin-5-one (110 mg, 0.29 mmol) was dissolved in neat DAST (1 mL), and the mixture was heated to 70 °C. After 4 h, the mixture was concentrated in vacuo and partitioned between DCM and water. The organic layer was dried (Na_2SO_4), concentrated, and purified via column chromatography to give 27 mg (23%) of 2-amino-8-(difluoro(pyridin-3-yl)methyl)-4-phenyl-5H-indeno[1,2-d]pyrimidin-5-one (**12**). $R_t = 4.10$ min. $^1\text{H NMR}$ (400 MHz, DMSO- d_6): δ 8.89 (s, 1H), 8.78 (d, $J = 3.54$ Hz, 1H), 8.15 (br. s., 1H), 8.09 (d, $J = 7.58$ Hz, 2H), 8.01 (d, $J = 7.07$ Hz, 2H), 7.92 (d, $J = 7.58$ Hz, 1H), 7.78–7.84 (m, 2H), 7.47–7.63 (m, 4H) ppm. $^{13}\text{C NMR}$ (151 MHz, DMSO- d_6): δ 186.8, 175.3, 165.8, 165.5, 152.3, 146.8, 140.7, 138.5, 136.0, 134.1, 132.5, 132.4, 131.5, 130.7, 130.0, 128.2, 124.5, 124.3, 120.1, 117.8, 111.5 ppm. HRMS, m/z calcd for $\text{C}_{23}\text{H}_{15}\text{F}_2\text{N}_4\text{O}$ [(M + H) $^+$], 401.1208; found, 401.1196.

2-Amino-8-(4-methylpiperazine-1-carbonyl)-4-phenyl-5H-indeno[1,2-d]pyrimidin-5-one (13). Neat piperazine (0.4 mL, 3.6 mmol) was added to a THF solution (60 mL) of acid **21** (1.7 g, 3.3 mmol), diisopropylethylamine (1.7 mL, 9.9 mmol), and HATU (1.3 g, 3.3 mmol). The resulting mixture was heated to 40 °C. After 18 h, the mixture was concentrated and purified via column chromatography to give 1.8 g (91%) of bis-*tert*-butyl (8-(4-methylpiperazine-1-carbonyl)-5-oxo-4-phenyl-5H-indeno[1,2-d]pyrimidin-2-yl)carbamate that was used immediately. The bis-*tert*-butyl (8-(4-methylpiperazine-1-carbonyl)-5-oxo-4-phenyl-5H-indeno[1,2-d]pyrimidin-2-yl)carbamate (1.8 g, 3.0 mmol) was then stirred in 25 mL of $\text{CH}_2\text{Cl}_2/\text{TFA}$ (4:1). After 3 h, the mixture was concentrated, neutralized with saturated aqueous NaHCO_3 , and filtered to give 1 g of crude 2-amino-8-(4-methylpiperazine-1-carbonyl)-4-phenyl-5H-indeno[1,2-d]pyrimidin-5-one (**13**). The solid was purified via column chromatography to give 893 mg (75%) of **13** as the free base, which was dissolved in THF and added to 10 mL of 1 N HCl in ether, concentrated, and dried in vacuo to give 2-amino-8-(4-methylpiperazine-1-carbonyl)-4-phenyl-5H-indeno[1,2-d]pyrimidin-5-one (**13**) as the di-HCl salt. $R_t = 2.63$ min. $^1\text{H NMR}$ (400 MHz, chloroform- d): δ ppm 2.34 (s, 3 H), 2.39 (br. s., 2 H), 2.52 (d, $J = 2.20$ Hz, 2 H), 3.46 (br. s., 2 H), 3.84 (br. s., 2 H), 5.86 (br. s., 2 H), 7.46–7.64 (m, 4 H), 7.78 (d, $J = 7.58$ Hz, 1 H), 7.85 (s, 1 H), 8.07 (dd, $J = 7.83, 1.71$ Hz, 2 H) ppm. $^{13}\text{C NMR}$ (101 MHz, DMSO- d_6): δ 186.5, 175.1, 167.8, 165.0, 164.9, 140.2, 139.6, 137.0, 135.5, 131.5, 130.9, 129.4, 127.6, 123.2, 119.3, 110.9, 57.1, 51.3, 42.2 ppm. HRMS, m/z calcd for $\text{C}_{23}\text{H}_{22}\text{N}_5\text{O}_2$ [(M + H) $^+$], 400.1768; found, 400.1780.

2-Amino-8-(2-morpholinoethoxy)-4-phenyl-5H-indeno[1,2-d]pyrimidin-5-one (14). Solid potassium *tert*-butoxide (*t*-BuOK) (9.7 g, 86.5 mmol) was added to a DMF solution (200 mL) of **25** (10.0 g, 34.6 mmol) and 4-(2-chloroethyl)morpholine hydrochloride (7.1 g, 38.1 mmol), and the resulting solution was heated to 75 °C. After 4 h at 75 °C, the mixture was cooled to room temperature diluted with tetrahydrofuran (THF) and EtOAc and washed with brine, water, and

brine. The organics were dried over Na_2SO_4 and dry packed onto silica gel. Column chromatography gave 7.0 g (50%) of the desired ether **14** as the free base, which was dissolved in THF and added to 100 mL of 2 N HCl in ether, concentrated, and dried in vacuo to give 2-amino-8-(2-morpholinoethoxy)-4-phenyl-5H-indeno[1,2-*d*]pyrimidin-5-one (**14**) as the di-HCl salt. $R_t = 2.85$ min. ^1H NMR (300 MHz, chloroform-*d*): δ ppm 2.53–2.67 (m, 4 H), 2.86 (t, $J = 5.65$ Hz, 2 H), 3.66–3.83 (m, 4 H), 4.25 (t, $J = 5.65$ Hz, 2 H), 5.76 (br. s., 2 H), 7.01 (dd, $J = 8.10, 2.45$ Hz, 1 H), 7.35 (d, $J = 2.26$ Hz, 1 H), 7.43–7.57 (m, 3 H), 7.66 (d, $J = 8.29$ Hz, 1 H), 7.98–8.10 (m, 2 H) ppm. ^{13}C NMR (101 MHz, DMSO-*d*₆): δ 186.2, 174.9, 164.1, 163.1, 162.4, 141.8, 134.6, 131.0, 129.5, 127.7, 125.0, 118.7, 111.5, 107.2, 63.0, 62.7, 54.5, 51.5 ppm. HRMS, m/z calcd for $\text{C}_{23}\text{H}_{23}\text{N}_4\text{O}_3$ [(M + H)⁺], 403.1765; found, 403.1754.

2-((Bis-*tert*-butoxycarbonyl)amino)-5-oxo-4-phenyl-5H-indeno[1,2-*d*]pyrimidine-8-carboxylic Acid (**21**). Solid *N*-methyl morpholine *N*-oxide (2.5 g, 21.2 mmol) was added to a CH_3CN solution (300 mL) of **7** (6.0 g, 10.6 mmol) and 4 Å ms (10.5 g). After 18 h at room temperature, the mixture was filtered, and the filtrate was diluted with EtOAc and washed with water and brine, dried (Na_2SO_4), and purified via column chromatography to give 3.6 g (68%) of bis-*tert*-butyl (8-formyl-5-oxo-4-phenyl-5H-indeno[1,2-*d*]pyrimidin-2-yl)carbamate. $R_t = 6.81$ min. ^1H NMR (400 MHz, chloroform-*d*): δ 10.17 (s, 1H), 8.43 (s, 1H), 8.24 (d, $J = 7.07$ Hz, 2H), 8.13 (d, $J = 7.58$ Hz, 1H), 7.96 (d, $J = 7.58$ Hz, 1H), 7.49–7.63 (m, 3H), 1.55 (s, 18H) ppm. ^{13}C NMR (101 MHz, chloroform-*d*): δ 190.6, 188.0, 175.3, 150.3, 141.2, 139.3, 134.8, 134.3, 132.3, 130.3, 128.3, 124.7, 122.6, 84.2, 77.3, 77.2, 77.0, 76.7, 27.9 ppm. HRMS, m/z calcd for $\text{C}_{28}\text{H}_{28}\text{N}_3\text{O}_6$ [(M + H)⁺], 502.1973; found, 502.1995.

Solid KMnO_4 was added to an acetone/water solution (100 mL/25 mL) of bis-*tert*-butyl (8-formyl-5-oxo-4-phenyl-5H-indeno[1,2-*d*]pyrimidin-2-yl)carbamate (3.6 g, 7.2 mmol), and the resulting mixture was heated to 55 °C. After 14 h, the mixture was cooled to room temperature and filtered. The filtrate was diluted with EtOAc and washed with water and brine, dried (Na_2SO_4), concentrated, and purified by column chromatography to give 2.1 g (57%) of 2-((bis-*tert*-butoxycarbonyl)amino)-5-oxo-4-phenyl-5H-indeno[1,2-*d*]pyrimidine-8-carboxylic acid (**21**). $R_t = 6.00$ min. ^1H NMR (400 MHz, chloroform-*d*): δ 8.54–8.65 (m, 1H), 8.26–8.36 (m, 1H), 8.17–8.24 (m, 2H), 7.78–7.89 (m, 1H), 7.48–7.63 (m, 3H), 1.53 (s, 18H) ppm. ^{13}C NMR (101 MHz, DMSO-*d*₆): δ 187.5, 175.0, 163.7, 163.3, 160.4, 159.9, 150.0, 134.9, 134.0, 131.6, 130.0, 129.9, 128.2, 127.9, 124.3, 118.7, 83.9, 27.3 ppm. HRMS, m/z calcd for $\text{C}_{28}\text{H}_{28}\text{N}_3\text{O}_7$ [(M + H)⁺], 518.1922; found, 518.1887.

(*E*)-2-Benzylidene-6-methoxy-2,3-dihydro-1H-inden-1-one (**23**). An aqueous solution (5 mL) of NaOH (1.5 g, 38.5 mmol) was added dropwise to an ethanol (EtOH) solution (30 mL) of 6-methoxy-1-indanone (5.0 g, 30.8 mmol) and benzaldehyde (3.4 g, 32.4 mmol). A precipitate formed immediately. An additional 3.0 mL of EtOH was added, and the resulting slurry was stirred vigorously for 0.5 h. The slurry was cooled in an ice bath, filtered, and washed with cold EtOH. The collected solid was dried in vacuo to give 7.3 g (95%) of (*E*)-2-benzylidene-6-methoxy-2,3-dihydro-1H-inden-1-one (**23**). $R_t = 5.39$ min. ^1H NMR (400 MHz, DMSO-*d*₆): δ 7.79 (d, $J = 7.07$ Hz, 2H), 7.59 (d, $J = 8.08$ Hz, 1H), 7.43–7.56 (m, 4H), 7.31 (dd, $J = 2.53, 8.08$ Hz, 1H), 7.26 (d, $J = 2.53$ Hz, 1H), 4.06 (s, 2H), 3.84 (s, 3H) ppm. ^{13}C NMR (101 MHz, DMSO-*d*₆): δ 193.1, 159.1, 142.6, 138.4, 135.8, 134.8, 132.6, 130.7, 129.7, 128.9, 127.5, 123.4, 105.5, 55.4, 31.1 ppm. HRMS, m/z calcd for $\text{C}_{17}\text{H}_{15}\text{O}_2$ [(M + H)⁺], 251.1067; found, 251.1056.

2-Amino-8-methoxy-4-phenyl-5H-indeno[1,2-*d*]pyrimidin-5-one (**24**). Powdered NaOH (5.8 g, 146.0 mmol) was added to an EtOH solution (130 mL) of guanidine acetate (17.4 g, 146.0 mmol). After 30 min, the sodium acetate (NaOAc) was filtered off, and the filtrate was added to an EtOH suspension (80 mL) of **23** (7.3 g, 29.2 mmol). The resulting mixture was heated to reflux overnight. The homogeneous solution was cooled in ice for 30 min and filtered to give 6.0 g of crude material (*des*-ketone), which was used without further purification. The crude material (6.0 g) was dissolved in NMP (80 mL), and powdered NaOH (1.2 g, 31.1 mmol) was added. The resulting mixture

was heated to 80 °C and air was bubbled through the solution using a steel needle. After 16 h, the mixture was cooled to room temperature, water was added, and the resulting precipitate was filtered and washed with water and cold EtOH. The red solid was dried in vacuo to give 5.0 g (56%) of 2-amino-8-methoxy-4-phenyl-5H-indeno[1,2-*d*]pyrimidin-5-one (**24**). $R_t = 4.04$ min. ^1H NMR (400 MHz, DMSO-*d*₆): δ 8.00 (d, $J = 6.57$ Hz, 2H), 7.92 (br. s., 2H), 7.62 (d, $J = 8.59$ Hz, 1H), 7.45–7.58 (m, 3H), 7.27 (d, $J = 2.53$ Hz, 1H), 7.15 (dd, $J = 2.53, 8.08$ Hz, 1H), 3.93 (s, 3H) ppm. ^{13}C NMR (101 MHz, DMSO-*d*₆): δ 186.5, 174.8, 164.8, 164.2, 164.1, 142.1, 135.6, 130.6, 129.5, 128.7, 127.5, 124.9, 117.7, 111.5, 106.1, 55.9 ppm. HRMS, m/z calcd for $\text{C}_{18}\text{H}_{14}\text{N}_3\text{O}_2$ [(M + H)⁺], 304.1081; found, 304.1065.

2-Amino-8-hydroxy-4-phenyl-5H-indeno[1,2-*d*]pyrimidin-5-one (**25**). An NMP solution (25 mL) of **24** (4.0 g, 13.2 mmol), LiCl (5.6 g, 132.0 mmol), and water (0.5 mL) were heated to 180 °C. After 4 h, the mixture was diluted with THF and EtOAc, washed with water and brine, dried (Na_2SO_4), filtered, and dry packed onto silica gel. Column chromatography gave 2.4 g (63%) of 2-amino-8-hydroxy-4-phenyl-5H-indeno[1,2-*d*]pyrimidin-5-one (**25**). $R_t = 3.58$ min. ^1H NMR (400 MHz, DMSO-*d*₆): δ 10.76 (s, 1H), 7.99 (d, $J = 6.57$ Hz, 2H), 7.87 (br. s., 2H), 7.42–7.59 (m, 4H), 7.15 (d, $J = 2.02$ Hz, 1H), 6.95 (dd, $J = 2.02, 8.08$ Hz, 1H) ppm. ^{13}C NMR (101 MHz, DMSO-*d*₆): δ 186.7, 175.0, 164.9, 163.9, 163.2, 142.4, 135.7, 130.6, 129.5, 127.6, 127.4, 125.3, 118.8, 111.6, 107.9 ppm. HRMS, m/z calcd for $\text{C}_{17}\text{H}_{12}\text{N}_3\text{O}_2$ [(M + H)⁺], 290.0924; found, 290.0923.

Pharmacokinetic Studies. Compound **1**, **13**, or **14** was administered to fasted Sprague–Dawley rats (male), Balb/c mice (male), and Cynomolus monkeys (male and female) by a single iv or oral administration. Compound **1** was formulated in 10% solutol for the iv injection. Compound **1** was formulated in 0.5% methylcellulose and dosed orally as a solution. The iv concentrations of **1** were 2 mg/kg for mice and rats and were 1 mg/kg for monkeys. The iv concentrations of **13** and **14** were 2 mg/kg for mice, rats, and monkeys. The oral concentrations of **1** were 10 mg/kg for all species. Discrete blood samples collected from mice and rats were withdrawn from 3 to 4 animals per time point at selected intervals postdose via orbital sinus (rats) or cardiac (mice) puncture. Serial blood collections from monkeys were withdrawn by venipuncture. Plasma was obtained by centrifugation, processed by acetonitrile precipitation, and then analyzed by LC-MS/MS. The limit of quantitation (LOQ) was 0.7–2 ng/mL. Noncompartmental analysis was performed on individual plasma concentrations using WinNonlin (version 4.0.4). For the tissue distribution studies, a 10 mg/kg solution of **1**, **13**, or **14** in 0.5% methylcellulose was administered orally to fasted Sprague–Dawley rats (male). At each time point, four animals were euthanized for collection of blood, plasma, and brain. Each tissue was weighed and homogenized in methanol. The methanolic extracts were evaporated and then reconstituted in mobile phase for analysis by LC-MS/MS. Blood and plasma were treated with acetonitrile, and the supernatants were analyzed for drug concentration by LC-MS/MS.

Mouse Catalepsy Study. Haloperidol, a neuroleptic medication that inhibits D_2 receptors, was used to induce catalepsy. In the rodent, catalepsy is characterized as a loss of voluntary motion where limbs uncharacteristically remain in placed positions. Catalepsy was measured in haloperidol (1 mg/kg, sc)-treated mice (fasted, male Balb/c mice) after oral administration of **1** (0.01, 0.10, 1.0, or 10.0 mg/kg, po), L-DOPA [300 mg/kg; coadministered with carbidopa (75 mg/kg)], or vehicle. Compounds **4–14** were given orally at 10 mg/kg to the haloperidol-treated mice using **1** (10 mg/kg, po) as the positive control, and the data were reported as the percent reversal of catalepsy. Dose responses of catalepsy were measured in haloperidol (1 mg/kg, sc)-treated mice (fasted, male Balb/c mice) after oral administration **4**, **5**, **6**, **13**, or **14** (0.1, 1.0, 3.0, or 10.0 mg/kg, po), **1** (10 mg/kg, po), or vehicle. Animals were randomly assigned to treatment groups, and behavioral testing was performed blind to treatment. Control mice received the respective sc and po vehicles. Haloperidol was dissolved in 0.3% tartaric acid in 0.9% saline. L-DOPA was diluted in 0.5% methylcellulose and dosed as a suspension. Compounds **1**, **13**, and **14** were diluted in 0.5% methylcellulose and dosed orally. Compounds **1**, **13**, and **14** were administered orally 30 min after haloperidol.

Behavioral testing was conducted 1 h after dosing of **1**, **13**, and **14**. The behavioral test trial (maximum duration of 60 s) began by placing the forepaws of fasted, male Balb/c mice on a horizontal bar elevated 3.5 cm above the bench. The cataleptic state was regarded as over, and the trial ended when the animal came off the bar by either placing its forepaws on the bench or climbing onto the bar with all of its limbs. Each value represents average (\pm SEM) time in cataleptic position of $n = 8$ – 12 mice per treatment group during a 60 s test session. Asterisks indicate significant differences as compared with the haloperidol + vehicle control group ($***P < 0.001$, Dunnett's test of multiple comparisons).

A separate study was performed using the same model of neuroleptic-induced catalepsy to examine the duration of action of **13** and **14** in mice. Catalepsy time was measured in haloperidol (1 mg/kg, sc)-treated mice (fasted, male Balb/c mice) after oral administration of **13** (0 or 10 mg/kg), **14** (0 or 10 mg/kg), **1** (10 mg/kg), or vehicle. Compounds **1**, **13**, and **14** were diluted in 0.5% methylcellulose. Catalepsy was measured repeatedly 30 min and 1, 2, and 4 h after oral dosing of the respective groups. Each value represents average (\pm SEM) time in cataleptic position of $n = 8$ mice per treatment group during a 60 s test session. Asterisks indicate significant differences as compared with the haloperidol + vehicle control group ($***P < 0.001$, Dunnett's test of multiple comparisons).

Rat Catalepsy Study. Haloperidol, a neuroleptic medication that inhibits D_2 receptors, was used to induce catalepsy. In the rodent, catalepsy is characterized as a loss of voluntary motion where limbs remain in placed positions. The time to descend from the bar was measured in haloperidol (1 mg/kg, sc)-treated male Sprague–Dawley rats (fasted) after oral administration of **13** or **14** (0.10, 1.0, 3.0, or 10.0 mg/kg), **1** (10 mg/kg), or vehicle. Animals were randomly assigned to treatment groups, and behavioral testing was performed blind to treatment. Control rats received the respective sc and po vehicles. Haloperidol was dissolved in 0.3% tartaric acid in 0.9% saline. Compound **1** was diluted in 0.5% methylcellulose and dosed as a solution. Compounds **13** and **14** were diluted in 20% HP β CD and dosed as a solution. Compounds **1**, **13**, and **14** were administered orally 30 min after haloperidol. Behavioral testing was conducted 1 h after dosing of **1**, **13**, and **14**. The behavioral test trial (maximum duration of 180 s) began by placing the forepaws of male Sprague–Dawley rats on a horizontal bar elevated 3.5 cm above the bench. The cataleptic state was regarded as over, and the trial ended when the animal came off the bar by either placing its forepaws on the bench or climbing onto the bar with all of its limbs. Each value represents average (\pm SEM) time in cataleptic position of $n = 10$ – 16 rats per treatment group during a 180 s test session. Asterisks indicate significant differences as compared with the haloperidol + vehicle control group ($***P < 0.001$, Dunnett's test of multiple comparisons).

A separate study was performed using the same model of neuroleptic-induced catalepsy to examine the duration of action of **14** in rats. Catalepsy time was measured in haloperidol (1 mg/kg, sc)-treated rats (fasted, male Sprague–Dawley rats) after oral administration of **14** (0 or 1.0 mg/kg), **1** (10 mg/kg), or vehicle. Compound **1** was diluted in 0.5% methylcellulose and dosed as a solution. Compound **14** was diluted in 20% HP β CD and dosed as a solution. Compounds **1** and **14** were administered orally 30 min after haloperidol. Catalepsy was measured repeatedly 15 min and 1, 2, and 4 h after oral dosing of the respective groups. Each value represents average (\pm SEM) time in cataleptic position of $n = 10$ rats per treatment group during a 180 s test session. Asterisks indicate significant differences as compared with the haloperidol + vehicle control group ($***P < 0.001$, Dunnett's test of multiple comparisons).

Reserpine-Induced Akinesia Study in Mice. Reserpine is an alkaloid that depletes monoamines by inhibiting their vesicular uptake, resulting in a dramatic reduction of spontaneous locomotor activity (akinesia). Efficacy is defined as reversal of reserpine-induced akinesia. Locomotion was studied in open field activity boxes (L, 17.5 in; W, 17.5 in; and H, 12 in), each containing 20 equally spaced pairs of horizontal infrared photocell beams along one axis. The activity was measured automatically by a PC running the activity analysis software. One activity count corresponded to the consecutive interruption of

two infrared beams placed 2.5 cm apart and 2 cm above the cage floor, and the total distance traveled was quantified in cm. Locomotion was studied 60 min after oral administration of compound **13** or **14** (0.1, 1.0, 3.0, 6.0, and 30 mg/kg, po), **1** (10 mg/kg), or vehicle in mice that were pretreated with reserpine (0.6 mg/kg, sc) 18 h earlier. Mice used were fasted male CF-1 mice. Animals were randomly assigned to treatment groups. Control mice received the respective sc and po vehicles. Reserpine was diluted in 0.5% acetic acid in distilled water and dosed sc. Compounds **13**, **14**, and **1** were diluted in 0.5% methylcellulose and dosed as a solution. Reserpine produced a marked decrease in horizontal and vertical locomotor activity. As shown in Figure 6, reserpine-induced akinesia was reversed by **13** and **14** at 1.0, 3.0, 6.0, and 10 mg/kg, po. Akinesia was also reversed by **1** at 10 mg/kg as the positive control. In Figure 6, each value represents the mean (\pm SEM) of the total distance traveled of $n = 14$ – 16 mice per treatment group during the 30 min measurement period in the behavioral test session. Asterisks indicate significant differences as compared with the reserpine + vehicle control group ($**P < 0.01$, $***P < 0.001$, Hochberg test of multiple comparisons).

Reserpine-Induced Akinesia Study in Rats. Reserpine is an alkaloid that depletes monoamines by inhibiting their vesicular uptake, resulting in a dramatic reduction of spontaneous locomotor activity (akinesia). Efficacy is defined as reversal of reserpine-induced akinesia. Locomotion was studied in open field activity boxes (L, 17.5 in; W, 17.5 in; and H, 12 in), each containing 20 equally spaced pairs of horizontal infrared photocell beams along one axis. A PC running the activity analysis software measured activity automatically. One activity count corresponded to the consecutive interruption of two infrared beams placed 2.5 cm apart and 2 cm above the cage floor, and the total distance traveled was quantified in cm. Locomotion was studied 60 min after oral administration of **13** (0.1, 1.0, 3.0, 6.0, and 10 mg/kg, po), **14** (0.1, 1.0, 3.0, and 10 mg/kg, po), **1** (10 mg/kg), or vehicle in rats that were pretreated with reserpine (0.6 mg/kg, sc) 18 h earlier. Animals were randomly assigned to treatment groups. Control rats received the respective sc and po vehicles. Rats used were fasted, male Wistar rats. Reserpine was diluted in 1% acetic acid in distilled water, **13** and **14** were diluted in 20% HP β CD, and **1** was diluted in 0.5% methylcellulose. Reserpine produced a marked decrease in motor activity. As shown in Figure 6, reserpine-induced akinesia was reversed by **13** at 1.0, 3.0, 6.0, and 10 mg/kg, po, and by **14** at 1.0, 3.0, and 10 mg/kg, po. Akinesia was also reversed by **1** at 10 mg/kg as the positive control. In Figure 7, each value represents the mean (\pm SEM) of the total distance traveled of $n = 16$ – 18 rats per treatment group during the 60 min measurement period in the behavioral test session. Asterisks indicate significant differences as compared with the reserpine + vehicle control group ($*P < 0.05$, $**P < 0.01$, and $***P < 0.001$, Hochberg test of multiple comparisons).

Rat 6-OHDA Lesion Model of Drug-Induced Rotation. The neurotoxin 6-OHDA (12 μ g) is microinjected unilaterally in the medial forebrain bundle to produce a targeted degeneration of midbrain DA neurons in the pars compacta of the substantia nigra. Fasted, male Sprague–Dawley rats weighing 227–260 g at the time of surgery were used in this study. 6-OHDA-induced neurotoxicity is relatively selective for monoaminergic neurons because DA and noradrenergic transporters preferentially take it up. 6-OHDA accumulates in the cytosol of neurons and generates reactive oxygen species, which then inhibit mitochondrial respiratory enzymes leading to metabolic deficits and DA cell death. Degeneration of dopaminergic neurons in the injected side of the brain is accompanied by denervation-induced supersensitivity of postsynaptic DA receptors in the striatum of the lesioned side. An imbalance in DA activity between the two sides of the brain causes asymmetry in motor behavior that can be enhanced by drug treatment. For example, drugs that stimulate postsynaptic DA receptors produce and imbalance in DA signaling that favors the lesion side and induces rotation behavior (turning) toward the side opposite (contralateral to) the lesion side. Three weeks after administration of 6-OHDA, rats were challenged with drugs acting on the dopaminergic system and studied in a behavioral test chamber. Each animal was tethered to high-resolution optical sensor connected to an automated computerized system that quantifies circular motion.

One rotation count was defined as one 360° turn. To test the effects of neuronal loss on drug responsiveness, motor asymmetry was examined in a screening test with subcutaneous administration of a postsynaptic DA agonist, apomorphine (0.05 mg/kg, sc). This test was repeated 1 week later and then followed 2 weeks later with a behavioral test to L-DOPA (10 mg/kg, po) coadministered with carbidopa (2.5 mg/kg, po). Animals showing an average response of at least 125 contralateral rotations in 1 h after apomorphine were included in further studies. Sixteen animals selected equidistant from the median L-DOPA response were used to test the effects of compound **1** on rotational behavior. To exclude a priming effect of L-DOPA, L-DOPA [10 mg/kg, po, coadministered with carbidopa (2.5 mg/kg, po)] was administered alone or with each dose of **13** or **14** (0.1, 1.0, 3.0, 6.0, and 10.0 mg/kg, po) to all animals on separate testing days in a randomized order, with each rat serving as its own control. The effects of **13** and **14** alone were also studied in the model. This within-subjects repeated measure design was carried out with at least two nondrug days elapsing between drug-testing sessions. Control rats received the respective po vehicles. Compounds **13** and **14** were diluted in 20% HP β CD and dosed as solutions. L-DOPA and carbidopa were diluted in 0.5% methylcellulose and coadministered as suspensions. Each behavioral test session began with a 30 min interval of acclimation in the test chamber, followed by administration of **13**, **14**, or vehicle and measurement of behavior for 60 min. Thereafter, the behavioral effects of L-DOPA (coadministered with carbidopa) or vehicle were measured for 120 min. Each value represents the mean (\pm SEM) of total contralateral rotations of $n = 16$ rats per treatment group during the 2 h before and after L-DOPA administration. Asterisks indicate significant differences as compared with the L-DOPA + vehicle control treatment group (* $P < 0.05$, ** $P < 0.01$, and *** $P < 0.001$) Tukey's test of multiple comparisons).

AUTHOR INFORMATION

Corresponding Author

*Tel: 215-628-7047. Fax: 215-540-4612. E-mail: bshook@its.jnj.com.

ABBREVIATIONS USED

6-OHDA, 6-hydroxydopamine; MPTP, 1-methyl-4-phenyl-1,2,3,6-tetrahydropyridine; PD, Parkinson's disease; DA, dopamine; L-DOPA, levodopamine; MAO-B, monoamine oxidase type B; COMT, catechol *O*-methyl-transferase; cAMP, cyclic adenosine monophosphate; PK, pharmacokinetics; PET, positron emission tomography; DMAP, 4-(dimethylamino)pyridine

REFERENCES

- (1) Lozano, A. M.; Lang, A. E.; Hutchison, W. D.; Dostrovsky, J. O. New developments in understanding the etiology of Parkinson's disease and in its treatment. *Curr. Opin. Neurobiol.* **1998**, *8*, 783–790.
- (2) Fink, J. S.; Weaver, D. R.; Rivkees, S. A.; Peterfreund, R. A.; Pollack, A. E.; Adler, E. M.; Reppert, S. M. Molecular cloning of the rat A₂ adenosine receptor: Selective co-expression with D₂ dopamine receptors in rat striatum. *Mol. Brain Res.* **1992**, *14*, 186–195.
- (3) Schiffmann, S. N.; Lipert, F.; Vassart, G.; Vanderhaeghen, J. J. Distribution of adenosine A₂ receptor mRNA in the human brain. *Neurosci. Lett.* **1991**, *130*, 177–181.
- (4) Olanow, C. W. MAO-B inhibitors in Parkinson's disease. *Adv. Neurol.* **1993**, *60*, 666–671.
- (5) (a) Gordin, A.; Brooks, D. J. Clinical pharmacology and therapeutic use of COMT inhibition in Parkinson's disease. *J. Neurol.* **2007**, *254*, IV/37–IV/48. (b) Olanow, C. W.; Stocchi, F. COMT inhibitors in Parkinson's disease. Can they prevent and/or reverse levodopa-induced motor complications? *Neurology* **2004**, *62*, S72–S81.
- (6) (a) Ramlackhansingh, A. F.; Bose, S. K.; Ahmed, I.; Turkheimer, F. E.; Pavese, N.; Brooks, D. J. Adenosine A_{2A} receptor availability in

dyskinetic and nondyskinetic patients with Parkinson's disease. *Neurology* **2011**, *76*, 1811–1816. (b) Antonini, A.; Clilia, R. Behavioural adverse effects of dopaminergic treatments in Parkinson's disease: Incidence, neurobiological basis, management and prevention. *Drug Saf.* **2009**, *32*, 475–488. (c) Hansard, M. J.; Smith, L. A.; Jackson, M. J.; Cheetham, S. C.; Jenner, P. Dopamine, but not norepinephrine or serotonin reuptake inhibition reverses motor deficits in 1-methyl-4-phenyl-1,2,3,6-tetrahydropyridine-treated primates. *J. Pharmacol. Exp. Ther.* **2002**, *303*, 952–958.

(7) (a) Antonini, A.; Tolosa, E.; Mizuno, Y.; Yamamoto, M.; Poewe, W. H. A reassessment of risks and benefits of dopamine agonists in Parkinson's disease. *Lancet Neurol.* **2009**, *8*, 929–937. (b) Yamamoto, M.; Schapira, A. H. V. Dopamine agonists in Parkinson's disease. *Expert Rev. Neurother.* **2008**, *8*, 671–677.

(8) (a) Shook, B. C.; Jackson, P. F. Adenosine A_{2A} receptor antagonists and Parkinson's disease. *ACS Chem. Neurosci.* **2011**, *2*, 555–567. (b) Neustadt, B. R.; Liu, H.; Hao, J.; Greenlee, W. J.; Stamford, A. W.; Foster, C.; Arik, L.; Lachowicz, J.; Zhang, H.; Bertorelli, R.; Fredduzzi, S.; Varty, G.; Cohen-Williams, M.; Ng, K. Potent and selective adenosine A_{2A} antagonists 1,2,4-triazolo[1,5-c]pyrimidines. *Bioorg. Med. Chem. Lett.* **2009**, *19*, 967–971. (c) Slee, D. H.; Zhang, X.; Moorjani, M.; Lin, E.; Lanier, M. C.; Chen, Y.; Rueter, J. K.; Lechner, S. M.; Markison, S.; Malany, S.; Joswig, T.; Santos, M.; Gross, R. S.; Williams, J. P.; Castro-Palomino, J. C.; Crespo, M. I.; Prat, M.; Gual, S.; Diaz, J. L.; Wen, J.; O'Brien, Z.; Saunders, J. Identification of novel, water soluble, 2-amino-N-pyrimidin-4-ylacetamides as A_{2A} receptor antagonists with in vivo activity. *J. Med. Chem.* **2008**, *51*, 400–406. (d) Shao, Y.; Cole, A. G.; Brescia, M. R.; Qin, L. Y.; Duo, J.; Stauffer, T. M.; Rokosz, L. L.; McGuinness, B. F.; Henderson, I. Synthesis and SAR studies of trisubstituted purinones as potent and selective adenosine A_{2A} receptor antagonists. *Bioorg. Med. Chem. Lett.* **2009**, *19*, 1399–1402. (e) Vu, C. B.; Peng, B.; Kumaravel, G.; Smits, G.; Jin, X.; Phadke, D.; Engber, T.; Huang, C.; Reilly, J.; Tam, S.; Grant, D.; Hetu, G.; Chen, L.; Zhang, J.; Pette, R. C. Piperazine derivatives of 1,2,4-triazolo[1,5-a][1,3,5]triazine as potent and selective adenosine A_{2A} receptor antagonists. *J. Med. Chem.* **2004**, *47*, 4291–4299.

(9) (a) Latini, S.; Pedata, F. Adenosine in the central nervous system: release mechanisms and extracellular concentrations. *J. Neurochem.* **2001**, *79*, 463–484. (b) Dunwiddie, T. V.; Masino, S. A. The role and regulation of adenosine in the central nervous system. *Annu. Rev. Neurosci.* **2001**, *24*, 31–55.

(10) Stiles, G. L. Adenosine receptors. *J. Biol. Chem.* **1992**, *267*, 6451–6454.

(11) (a) Rosin, D. L.; Robeva, A.; Woodard, R. L.; Guyenet, P. G.; Linden, J. Immunohistochemical localization of adenosine A_{2A} receptors in rat central nervous system. *J. Comp. Neurol.* **1998**, *401*, 163–186. (b) Fredholm, B. B.; Svenningsson, P. Striatal adenosine A_{2A} receptors—where are they? What do they do? *Trends Pharmacol. Sci.* **1998**, *19*, 46–47.

(12) (a) Ishiwata, K.; Mishina, M.; Kimura, Y.; Oda, K.; Sasaki, T.; Ishii, K. First visualization of adenosine A_{2A} receptors in the human brain by positron emission tomography with [¹¹C]TMSX. *Synapse* **2005**, *55*, 133–136. (b) Svenningsson, P.; Hall, H.; Sedvall, G.; Fredholm, B. B. Distribution of adenosine receptors in the postmortem human brain: an extended autoradiographic study. *Synapse* **1997**, *27*, 322–335.

(13) Varani, K.; Vincenzi, F.; Tosi, A.; Gessi, S.; Casetta, I.; Granieri, G.; Fazio, P.; Leung, E.; MacLennan, S.; Granieri, E.; Borea, P. A. A_{2A} adenosine receptor overexpression and functionality, as well as TNF- α levels, correlate with motor symptoms in Parkinson's disease. *FASEB J.* **2010**, *24*, S87–S98.

(14) Pollack, A. E.; Fink, J. S. Adenosine antagonists potentiate D2 dopamine dependent activation of Fos in the striatopallidal pathway. *Neuroscience* **1995**, *68*, 721–728.

(15) Duty, S.; Jenner, P. Animal models of Parkinson's disease: A source of novel treatments and clues to the cause of the disease. *Br. J. Pharmacol.* **2011**, *164*, 1357–1391.

- (16) (a) Chen, J. F.; Xu, K.; Petzer, J. P.; Staal, R.; Xu, Y. H.; Beilstein, M.; Sonsalla, P. K.; Castagnoli, K.; Castagnoli, N.; Schwarzchild, M. A. Neuroprotection by caffeine and A_{2A} adenosine receptor inactivation in a model of Parkinson's disease. *J. Neurosci.* **2001**, *21*, RC143/1–RC143/6. (b) Grondin, R.; Bedard, P. J.; Tahar, A. J.; Gregoire, L.; Mori, A.; Kase, H. Antiparkinsonian effect of a new adenosine A_{2A} receptor antagonist in MPTP-treated monkeys. *Neurology* **1999**, *52*, 1673–1677. (c) Ongini, E.; Monopoli, A.; Impagnatiello, F.; Fredduzzi, S.; Schwarzchild, M.; Chen, J. F. Dual actions of A_{2A} adenosine receptor antagonists on motor dysfunction and neurodegenerative processes. *Drug Dev. Res.* **2001**, *52*, 379–386. (d) Ikeda, K.; Kurokawa, M.; Aoyama, S.; Kuwana, Y. Neuroprotection by adenosine A_{2A} receptor blockade in experimental models of Parkinson's disease. *J. Neurochem.* **2002**, *80*, 262–270.
- (17) (a) Kanda, T.; Jackson, M. J.; Smith, L. A.; Pearce, R. K. B.; Nakamura, J.; Kase, H.; Kuwana, Y.; Jenner, P. Adenosine A_{2A} antagonist: a novel antiparkinsonian agent that does not provoke dyskinesia in parkinsonian monkeys. *Ann. Neurol.* **1998**, *43*, 507–513. (b) Koga, K.; Kurokawa, M.; Ochi, M.; Nakamura, J.; Kuwana, Y. Adenosine A_{2A} receptor antagonists KF17837 and KW-6002 potentiate rotation induced by dopaminergic drugs in hemi-Parkinsonian rats. *Eur. J. Pharmacol.* **2000**, *408*, 249–255.
- (18) (a) Neustadt, B. R.; Hao, J.; Lindo, N.; Greenlee, W. J.; Stamford, A. W.; Tulshian, D.; Ongini, E.; Hunter, J.; Monopoli, A.; Bertorelli, R.; Foster, C.; Arik, L.; Lachowicz, J.; Ng, K.; Feng, K. I. Potent, selective, and orally active adenosine A_{2A} receptor antagonists: arylpiperazine derivatives of pyrazolo[4,3-e]-1,2,4-triazolo[1,5-c]-pyrimidines. *Bioorg. Med. Chem. Lett.* **2007**, *17*, 1376–1380. (b) Hodgson, R. A.; Bertorelli, R.; Varty, G. B.; Lachowicz, J. E.; Forlani, A.; Fredduzzi, S.; Cohen-Williams, M. E.; Higgins, G. A.; Impagnatiello, F.; Nicolussi, E.; Parra, L. E.; Foster, C.; Zhai, Y.; Neustadt, B. R.; Stamford, A. W.; Parker, E. M.; Reggiani, A.; Hunter, J. C. Characterization of the potent and highly selective A_{2A} receptor antagonists preladenant and SCH 412348 [7-[2-[4-(2,4-difluorophenyl)-1-piperazinyl]ethyl]-2-(2-furanyl)-7H-pyrazolo[4,3-e][1,2,4]-triazolo[1,5-c]pyrimidin-5-amine] in rodent models of movement disorders and depression. *J. Pharmacol. Exp. Ther.* **2009**, *330*, 294–303.
- (19) (a) Kanda, T.; Jackson, M. J.; Smith, L. A.; Pearce, R. K.; Nakamura, J.; Kase, H.; Kuwana, Y.; Jenner, P. Combined use of the adenosine A_{2A} antagonist KW-6002 with L-DOPA or with selective D_1 or D_2 dopamine agonists increases antiparkinsonian activity but not dyskinesia in MPTP-treated monkeys. *Exp. Neurol.* **2000**, *162*, 321–327. (b) Hauser, R. A.; Hubble, J. P.; Truong, D. D. Randomized trial of adenosine A_{2A} receptor antagonist istradefylline in advanced PD. *Neurology* **2003**, *61*, 297–303. (c) Bara-Jimenez, W.; Sherzai, A.; Dimitrova, T.; Favit, A.; Bibbiani, F.; Gillespie, M.; Morris, M. J.; Mouradian, M. M.; Chase, T. N. Adenosine A_{2A} receptor antagonist treatment of Parkinson's disease. *Neurology* **2003**, *61*, 293–296.
- (20) For the current status of preladenant, go to clinicaltrials.gov and use the following identifiers: NCT01155479, NCT01227265, NCT01155466, NCT01294800, NCT01215227, and NCT01323855.
- (21) Kimura, Y.; Ishii, K.; Fukumitsu, N.; Oda, K.; Sasaki, T.; Kawamura, K.; Ishiwata, K. Quantitative analysis of adenosine A_1 receptors in human brain using positron emission tomography and [1-methyl- ^{11}C]8-dicyclopropylmethyl-1-methyl-3-propylxanthine. *Nuclear Med. Biol.* **2004**, *31*, 975–981.
- (22) Ballarin, M.; Reiriz, J.; Ambrosio, S.; Mahy, N. Effect of locally infused 2-cholroadenosine, an A_1 receptor agonist, on spontaneous and evoked dopamine release in rat neostriatum. *Neurosci. Lett.* **1995**, *185*, 29–32.
- (23) (a) Moore, K. A.; Nicoll, R. A.; Schmitz, D. Adenosine gates synaptic plasticity at hippocampal mossy fiber synapses. *Proc. Natl. Acad. Sci.* **2003**, *100*, 14397–14402. (b) Rebola, N.; Pinheiro, P. C.; Oliveira, C. R.; Malva, J. O.; Cunha, R. A. Subcellular localization of adenosine A_1 receptors in nerve terminal and synapses of the rat hippocampus. *Brain Res.* **2003**, *987*, 49–58.
- (24) Maemoto, T.; Miho, T.; Takuma, M.; Noriko, U.; Hideaki, M.; Katsuya, H.; Takayuki, Y.; Kiyoharu, S.; Satoru, K.; Atsushi, A.; Akinori, I.; Nobuya, M.; Seitaro, M. Pharmacological characterization of FR194921, a new potent, selective, orally active antagonist for central adenosine A_1 receptors. *J. Pharmacol. Sci.* **2004**, *96*, 42–52.
- (25) Yonishi, S.; Aoki, S.; Matsushima, Y.; Akahane, A. Preparation of pyrazines as adenosine A_1 and A_{2A} receptor antagonists and their pharmaceutical compositions. PCT Int. Appl. WO 2005040151, 2005.
- (26) (a) Mihara, T.; Iwashita, A.; Matsuoka, N. A novel adenosine A_1 and A_{2A} receptor antagonist ASP5854 ameliorates motor impairment in MPTP-treated marmosets: Comparison with existing anti-Parkinson's disease drugs. *Behav. Brain Res.* **2008**, *194*, 152–161. (b) Mihara, T.; Noda, A.; Arai, H.; Mihara, K.; Iwashita, A.; Murakami, Y.; Matsuya, T.; Miyoshi, S.; Nishimura, S.; Matsuoka, N. Brain adenosine A_{2A} receptor occupancy by a novel A_1/A_{2A} receptor antagonist, ASP5854, in rhesus monkeys: Relationship to antiepileptic effect. *J. Nucl. Med.* **2008**, *49*, 1183–1188.
- (27) Mihara, T.; Mihara, K.; Yarimizu, J.; Mitani, Y.; Matsuda, R.; Yamamoto, H.; Aoki, S.; Akahane, A.; Iwashita, A.; Matsuoka, N. Pharmacological characterization of a novel, potent adenosine A_1 and A_{2A} receptor dual antagonist, 5-[5-amino-3-(4-fluorophenyl)pyrazin-2-yl]-1-isopropylpyridine-2(1H)-one (ASP5854), in models of Parkinson's disease and cognition. *J. Pharmacol. Exp. Ther.* **2007**, *323*, 708–719.
- (28) (a) Shook, B. C.; Rassnick, S.; Osborne, M. C.; Davis, S.; Westover, L.; Boulet, J.; Hall, D.; Rupert, K. C.; Heintzelman, G. R.; Hansen, K.; Chakravarty, D.; Bullington, J. L.; Russell, R.; Branum, S.; Wells, K. M.; Damon, S.; Youells, S.; Li, X.; Beauchamp, D. A.; Palmer, D.; Reyes, M.; Demarest, K.; Tang, Y.-T.; Rhodes, K.; Jackson, P. F. In Vivo Characterization of a Dual Adenosine A_{2A}/A_1 Receptor Antagonist in Animal Models of Parkinson's Disease. *J. Med. Chem.* **2010**, *53*, 8104–8115. (b) Shook, B. C.; Rassnick, S.; Hall, D.; Rupert, K. C.; Heintzelman, G. R.; Hansen, K.; Chakravarty, D.; Bullington, J. L.; Scannevin, R.; Magliaro, B.; Westover, L.; Carroll, K.; Lampron, L.; Russell, R.; Branum, S.; Wells, K.; Damon, S.; Youells, S.; Li, X.; Osbourne, M.; Demarest, K.; Tang, Y.; Rhodes, K.; Jackson, P. F. Methylene amine substituted arylindolopyrimidines as potent adenosine A_{2A}/A_1 antagonists. *Bioorg. Med. Chem. Lett.* **2010**, *20*, 2864–2867. (c) Shook, B. C.; Rassnick, S.; Chakravarty, D.; Wallace, N.; Ault, M.; Crooke, J.; Barbay, J. K.; Wang, A.; Leonard, K.; Powell, M. T.; Alford, V.; Hall, D.; Rupert, K. C.; Heintzelman, G. R.; Hansen, K.; Bullington, J. L.; Scannevin, R.; Carroll, K.; Lampron, L.; Westover, L.; Russell, R.; Branum, S.; Wells, K.; Damon, S.; Youells, S.; Beauchamp, D.; Li, X.; Rhodes, K.; Jackson, P. F. Optimization of arylindolopyrimidines as potent adenosine A_{2A}/A_1 antagonists. *Bioorg. Med. Chem. Lett.* **2010**, *20*, 2868–2871.
- (29) Zarrindast, M. R.; Modabber, M.; Sabetkasai, M. Influence on different adenosine receptor subtypes on catalepsy in mice. *Psychopharmacology* **1993**, *113*, 257–261.
- (30) Mandhane, S. N.; Chopde, C. T.; Ghosh, A. K. Adenosine A_2 receptors modulate haloperidol-induced catalepsy in rats. *Eur. J. Pharmacol.* **1997**, *328* (2/3), 135–141.
- (31) Cooper, D. R.; Marrel, C.; van de Waterbeemd, H.; Testa, B.; Jenner, P.; Marsden, C. D. L-Dopa esters as potential prodrugs: Behavioral activity in experimental models of Parkinson's disease. *J. Pharm. Pharmacol.* **1987**, *39*, 627–635.
- (32) (a) Ungerstedt, U. 6-Hydroxydopamine-induced generation of central monoamine neurons. *Eur. J. Pharmacol.* **1968**, *5*, 107–110. (b) Ungerstedt, U.; Arbuthnott, G. W. Quantitative recording of rotational behavior in rats after 6-hydroxy-dopamine lesions of the nigrostriatal dopamine system. *Brain Res.* **1970**, *24*, 485–493. (c) Luthman, J.; Fredriksson, A.; Sundstroem, E.; Jonsson, G.; Archer, T. Selective lesion of central dopamine or moradenaline neuron systems in the neonatal rat: Motor behavior and monoamine alteration at adult stage. *Behav. Brain Res.* **1989**, *33*, 267–277.
- (33) (a) Bankiewicz, K. S. MPTP-induced parkinsonism in nonhuman primates. *Methods Neurosci.* **1991**, *7*, 168–182. (b) Jakowec, M. W.; Petzinger, G. M. 1-methyl-4-phenyl-1,2,3,6-tetrahydropyridine-induced lesion model of Parkinson's disease, with emphasis on mice and nonhuman primates. *Comp. Med.* **2004**, *54*, 497–513. (c) Campos-Romo, A.; Ojeda-Flores, R.; Moreno-Briseno, P.;

Fernandez-Ruiz, J. Quantitative evaluation of MPTP-treated nonhuman parkinsonian primates in the hallway task. *J. Neurosci. Methods* **2009**, *177*, 361–368.

(34) Lim, H.-K.; Chen, J.; Sensenhauser, C.; Cook, K.; Preston, R.; Thomas, T.; Shook, B.; Jackson, P. F.; Rassnick, S.; Rhodes, K.; Gopaul, V.; Salter, R.; Silva, J.; Evans, D. C. Overcoming the genotoxicity of a pyrrolidine substituted arylindenopyrimidine as a potent adenosine A_{2A}/A₁ antagonist by minimizing bioactivation to an iminium ion reactive intermediate. *Chem. Res. Toxicol.* **2011**, *24*, 1012–1030.

(35) Hyttel, J.; Larsen, J. J.; Christensen, A. V.; Arnt, J. Receptor-binding profiles of neuroleptics. *Psychopharmacol. Suppl.* **1985**, *2*, 9–18.

(36) Kraus, G. A.; Sy, J. O. A synthetic approach to rocaglamide via reductive cyclization of δ -keto nitriles. *J. Org. Chem.* **1989**, *54*, 77–83.

(37) Heintzelman, G. R.; Bullington, J. L.; Rupert, K. C. Preparation of arylindenopyridines and arylindenopyrimidines and their use as adenosine A_{2A} receptor antagonists. PCT Int. Appl. WO 2005042500, 2005.

(38) (a) Yu, Y.; Liebeskind, L. S. Copper-mediated, palladium-catalyzed coupling of thiol ester with aliphatic organoboron reagents. *J. Org. Chem.* **2004**, *69*, 3554–3557. (b) Kusturin, C.; Liebeskind, L. S.; Rahman, H.; Sample, K.; Schweitzer, B.; Srogl, J.; Neumann, W. L. Switchable catalysis: Modular synthesis of functionalized pyrimidones via selective sulfide and halide cross-coupling chemistry. *Org. Lett.* **2003**, *5*, 4349–4352. (c) Liebeskind, L. S.; Srogl, J. Heteroaromatic thioether-boronic acid cross-coupling under neutral reaction conditions. *Org. Lett.* **2002**, *4*, 979–981.

(39) (a) Marsden, C. D.; Dolphin, A.; Duvoisin, R. C.; Jenner, P.; Tarsy, D. Role of noradrenaline in levodopa reversal of reserpine akinesia. *Brain Res.* **1974**, *17*, 521–525. (b) Starr, M. S.; Starr, B. S. Comparison of the effects NMDA and AMPA antagonist on the locomotor activity induced by selective D₁ and D₂ dopamine agonists in reserpine-treated mice. *Psychopharmacology* **1994**, *114*, 495–504.

(40) Robinson, T. E.; Becker, J. B. The rotational behavior model: Asymmetry in the effects of unilateral 6-OHDA lesions of the substantia nigra in rats. *Brain Res.* **1983**, *264*, 127–131.

(41) Damier, P.; Hirsch, E. C.; Agid, Y.; Graybiel, A. M. The substantia nigra of the human brain. II. Patterns of loss of dopamine-containing neurons in Parkinson's disease. *Brain* **1999**, *122*, 1437–1448.